Biomechanical Analysis of Fall Injuries using Finite Element Modeling

Pooya Sahandifar

Doctoral Thesis
KTH Royal Institute of Technology
School of Engineering Science in Chemistry, Biotechnology, and Health
Neuronic Engineering
SE- 141 57 Huddinge, Sweden

TRITA-CBH-FOU-2022:29
ISBN 978-91-8040-211-8
The academic dissertation, with permission from Kungliga Tekniska Högskolan (Royal Institute of Technology) in Stockholm, is presented for public review for passing the doctoral examination on Monday, May 23rd, 2022, at 14:00 P.M. in room Rappesalen, Alfred Nobels Allé 10, Huddinge, Sweden.

To my loved ones who are the light at the end of the tunnel

Abstract

A fall is a serious health issue for the elderly. Among different fall types, the sideways fall is considered to be more severe concerning the injury outcome. When elderlies experience an unintentional sideways fall, they can either resist the impact forces with the soft tissue force attenuation capacity and femoral strength or need external protections to reduce the injury risk. In this thesis, these two aspects were investigated. Finite element whole-body models are valuable tools for analyzing fall biomechanics and investigating the possible preventive measures more conveniently. The whole-body models were developed to investigate traffic accidents; however, a sideways fall has different kinematics than the other types of accidents. Consequently, it is necessary to enhance the whole-body models according to the major fall parameters leading to severe injury cases before assessing the external protection capabilities.

The current thesis attempted to advance these two critical aspects regarding fall-induced injuries. A finite element whole-body model was chosen to study three critical parameters in fall biomechanics: body posture, soft tissue, and femoral strength. The whole body model was positioned in different body configurations relevant for the sideways fall to evaluate the body posture that could lead to the highest internal forces on the femoral head. Next, different soft tissue constitutive material models and soft tissue thicknesses were investigated to find a material model that could accurately reproduce the experimental results according to an objective rating method named CORrelation and Analysis (CORA). Finally, the separate and combined effects of geometrical and mechanical properties change due to aging on femoral strength were assessed for the elderly males and females. In the second aspect of the thesis, the shock-absorbing rubberized asphalt pavements' preventive capacity was examined. First, different rubberized asphalt mixtures were implemented in a bicycle and a pedestrian accident reconstruction cases to evaluate the head injury risks. Later, the asphalt mixtures were studied in a sideways fall scenario to evaluate the hip fracture risk in an elderly male and female.

The first aspect of the thesis presented the results and methods to improve the sideways fall analysis, and the second aspect of the thesis focused on assessing the rubberized asphalt mixtures for injury prevention purposes. The sideways fall with the upright trunk and a slightly forward-tilted pelvis could lead to the highest internal forces. A nonlinear Ogden material model for muscle tissue and a Mooney-Rivlin material model for adipose tissue scored better among different soft tissue material models in the side impacts to the hip segments. The geometrical and mechanical properties change due to aging leading to a different behavior for males and females, where females experience a higher rate of strength loss due to aging. Moreover, it was indicated that a rubberized asphalt mixture could reduce the head injury risk for pedestrians and cyclists and the hip fracture risk for the elderly. The amount of rubber in the asphalt mixtures needs to exceed a specific limit to observe rubberized asphalts' preventive effects. Consequently, it is necessary to optimize the mixtures' rubber content to improve its prevention capacity.

In summary, the current thesis presented a method to improve the whole-body models according to the sideways fall requirements and assessed the protective capacity of the rubberized asphalt mixtures against head and hip injuries.

Keywords
Fall induced injury, finite element analysis, rubberized asphalt mixture, shock-absorbing pavement, hip fracture, elderly, sideways fall, whole-body model

Sammanfattning

Ett fall är ett allvarligt hälsoproblem för äldre. Bland olika falltyper anses fallet i sidled vara allvarligare vad gäller skadeutfallet. När äldre drabbas av ett oavsiktligt fall i sidled kan de antingen stå emot slagkrafterna med mjukvävnadskraftens dämpningsförmåga och lårbensstyrka eller behöva yttre skydd för att minska skaderisken. I denna avhandling har dessa två aspekter undersökts. Finite element helkroppsmodeller är värdefulla verktyg för att analysera falls biomekanik och lämpligt för att undersöka möjliga förebyggande åtgärder mer bekvämt. Helkroppsmodellerna utvecklades för att undersöka trafikolyckorna; ett fall i sidled har dock en annan kinematik än de andra typerna av olyckor. Följaktligen är det nödvändigt att förbättra helkroppsmodellerna enligt de viktigaste fallparametrarna, vilket leder till allvarliga skadefall, innan man bedömer de yttre skyddsförmågan.

Den aktuella avhandlingen försökte föra fram dessa två kritiska aspekter angående fallinducerade skador. En finite element helkroppsmodell valdes för att studera tre kritiska parametrar i falls biomekanik: kroppshållning, mjukvävnad och femoral styrka. Helkroppsmodellen placerades i olika kroppskonfigurationer som är relevanta för fallet i sidled för att utvärdera kroppshållningen som kunde leda till de högsta inre krafterna på lårbenshuvudet. Därefter undersöktes olika konstitutiva materialmodeller för mjukvävnad och mjukdelstjocklekar för att hitta en materialmodell som exakt kunde återge de experimentella resultaten enligt en objektiv klassificeringsmetod som heter CORrelation and Analysis (CORA). Slutligen utvärderades de separata och kombinerade effekterna av förändringar av geometriska och mekaniska egenskaper på grund av åldrande på lårbensstyrkan för äldre män och kvinnor. I den andra aspekten av avhandlingen undersöktes de stötdämpande gummerade asfaltbeläggningarnas förebyggande kapacitet. Först implementerades olika gummerade asfaltblandningar i rekonstruktionsfallen för en cykel och en fotgängarolycka för att utvärdera riskerna för huvudskador. Senare studerades asfaltblandningarna i ett sidledes fallscenario för att utvärdera risken för höftfraktur hos en äldre man och kvinna.

Den första aspekten av avhandlingen presenterade resultaten och metoderna för att förbättra analysen av sidledsfall, och den andra aspekten av avhandlingen fokuserade på att bedöma de gummerade asfaltblandningarna i skadeförebyggande syfte. Fall i sidled med upprätt bål, och ett något framåtlutat bäcken kan leda till de högsta inre krafterna. En ickelinjär Ogden-materialmodell för muskelvävnad och en Mooney-Rivlin-materialmodell för fettvävnad fick bättre poäng bland olika mjukdelsmaterialmodeller i sidokollisioner mot höftsegmenten. De geometriska och mekaniska egenskaperna förändras på grund av åldrande vilket leder till ett annorlunda beteende för män och kvinnor där kvinnor upplever en högre grad av förlust i styrka på grund av åldrande. Dessutom indikerades att en gummerad asfaltblandning kunde minska risken för huvudskador för fotgängare och cyklister och risken för höftfraktur för äldre. Mängden gummi i asfaltblandningarna behöver överskrida en specifik gräns för att observera gummerad asfalts förebyggande effekt.

Följaktligen är det nödvändigt att optimera blandningarnas gummihalt för att förbättra dess förebyggande förmåga.

Sammanfattningsvis presenterade den aktuella avhandlingen en metod för att förbättra helkroppsmodellerna enligt kraven på sidledes fall och bedömde skyddsförmågan hos de gummerade asfaltblandningarna vid huvud- och höftskador.

Nyckelord
Fallinducerad skada, finit elementanalys, gummerad asfaltblandning, fallvänlig asfalt, höftfraktur, äldre, fall i sidled, helkroppsmodell

List of Appended Papers

Paper A
Kleiven, S., Sahandifar P. (2022). Upright trunk and slight anterior rotation of the pelvis cause the highest proximal femur forces during sideways falls. (Manuscript, submitted).

Paper B
Sahandifar P., Kleiven, S. (2021). Influence of nonlinear soft tissue modeling on the external and internal forces during lateral hip impacts. Journal of the Mechanical Behavior of Biomedical Materials (10.1016/j.jmbbm.2021.104743).

Paper C
Sahandifar P., Kleiven, S. (2021). Separate and Combined Effects of Geometrical and Mechanical Properties Changes Due to Aging on the Femoral Strength in Men and Women. Frontiers in Mechanical Engineering (10.3389/fmech.2021.691171).

Paper D
Sahandifar P., Makoundou C., Fahlstedt M., Sangiorgi C., Johansson K., Wallqvist V., Kleiven, S. (2022). A rubberized impact absorbing pavement can reduce the head injury risk in vulnerable road users: a bicycle and a pedestrian accident case study. Traffic Injury Prevention (10.1080/15389588.2022.2067990)

Paper E
Sahandifar P., Wallqvist V., Kleiven, S. (2022). The risk of hip fracture is reduced around 40 percent for elderly men and women with a compliant pavement. (manuscript).

Division of Work

Paper A
The study design was done by Svein Kleiven (SK). Pooya Sahandifar (PS) and SK performed the study. PS wrote the manuscript under the supervision of SK.

Paper B
The study design was done by PS and SK. PS performed the study and wrote the manuscript under the supervision of SK.

Paper C
The study design was done by PS and SK. PS performed and analyzed the finite element simulations and wrote the original draft. SK performed supervision, funding acquisition, writing review, and editing.

Paper D
The study design was done by PS, SK, Christina Makoundou (CM), and Cesare Sangiorgi (CS). CM and CS developed the soft asphalt samples. CM, Kenth Johansson (KJ) and Viveca Wallqvist (VW) performed the standard HIC drop test. PS and CM performed mechanical testing. PS assessed test results prepared the finite element models, and analyzed the finite element simulations. Madelen Fahlstedt (MF) provided the bicycle accident reconstruction. PS and CM wrote the original draft. SK, MF, CS, KJ, and VW performed supervision.

Paper E
The study design was done by PS and SK. PS performed this study and wrote the manuscript under the supervision of SK and VW.

Other Scientific Contributions

Conference Proceeding

Sahandifar P., Kleiven, S. (2018). Studying the age effect on fall-induced hip fracture using an orthotropic continuum damage model (Short communication). International Research Council on the Biomechanics of Injury, IRCOBI, 11-12 September, Athens, Greece.

Sahandifar P., Kleiven, S., Wallqvist V. (2020). Competence of soft asphalt for prevention of the fall induced injuries among vulnerable road users (Short communication). Transportforum 2020, 8-9 January, Väg-och transportforskningsinstitutet (VTI), Linköping, Sweden,http://vti.diva-portal.org/smash/get/diva2:1411216/FULLTEXT01.pdf

Preface and Acknowledgment

I was dreaming about being at Neuronics during my master thesis, and now I am finishing this amazing chapter of my life at Neuronics. During my Ph.D., I lived my dream, and I am very happy that this dream came true. Every success comes from a team that supported and assisted all the way toward the apex. I would like to use this opportunity to express my appreciation for this wonderful team.

I had a chance to work with two supervisors during my Ph.D., Professor Svein Kleiven and Dr. Viveca Wallqvist. Svein, it would be hard to reach this point without your supervision. I am thankful that you trusted my skills and boosted my confidence at the moments I felt lost. I learned doing research and improved day by day with your guidance. Viveca, from our first meeting till the latest, I continuously got insightful information not only about my project but also about the exciting projects you were involved in. It was always inspiring to share ideas about the forthcoming future that we, as a scientist or engineer, can build.

The Neuronics group has been dynamically changing since I started. I became a member of the group when Victor, Chiara, Qingling, Zhou, Shiyang, and Annaclaudia were Ph.D. students, and later new members, Reza, Teng, Qiantailang, and Natalia joined Neuronics. It was wonderful spending time with all of you and exchanging thoughts about our projects. I would like to thank our senior members, Xiaogai and Madelen, who always had open doors to assist. Beyond Neuronics, I found wonderful friends at CBH, David, Elira, Liyun, Jayanth, Vinutha, and Elhabib, who made being a Ph.D. student a pleasant experience. Abdolamir, Farhad, Shirin, and Mehdi, you became my new family when I was apart from my own. A special thanks to Daniel; you gave me a lot of motivation and energy. I became better at badminton and learned Innebandy with you.

I would like to thank two of my supervisors in my BSc and MSc projects at Sharif university of technology, Professor Reza Naghdabadi, and Professor Farzam Farahmand. I learned to pave the way ahead in engineering with your guidance. Professor Farahmand, thanks for talking about biomechanics in the first lecture of my bachelor's degree. It was a great opportunity to identify an aim to pursue from my first days of being a mechanical engineer. Professor Naghdabadi, thanks for giving me the opportunity to work on brain injuries which opened the door to my dreams about Neuronics.

And finally, my family. Mom, Dad, and Nima, no word can explain how much I missed you, and no word is enough to thank you for every second and minute. I achieved my goals with your help and sacrifices. Fatima, I am grateful to have you in my life. It was not easy to pave the way during my Ph.D. without you being by my side. I appreciate your efforts and assistance through the tough times. I love you.

The thesis was carried out at the Neuronic Engineering unit, KTH Royal Institute of Technology in Stockholm, Sweden. The thesis was funded by "BVFF – Bana väg för framtiden" (BVFF number 2016-025).

مامان، بابا، نیما و فاطمه از شما خیلی خیلی ممنونم و همه شما را از صمیم قلبم دوست دارم.

Stockholm, May 2022

Pooya Sahandifar

Abbreviations

BMD	Bone Mineral Density
BMI	Body Mass Index
CORA	CORrelation and Analysis
GHBMC	Global Human Body Models Consortium
HBM	Human Body Model
HIC	Head Injury Criterion
HR-pQCT	High Resolution-peripheral Quantitative Computed Tomography
QCT	Quantitative Computed Tomography
EPDM	Ethylene Propylene Diene Methyl
QLV	Quasilinear Viscoelastic Model
HU	Hysteresis Unloading
MPP	Massively Parallel Processing
SD	Standard Deviation
SMP	Shared Memory Parallel
THUMS	Total Human Model for Safety
VRU	Vulnerable Road Users
WHO	World health organization

Contents

1 Introduction

A fall can be defined differently among different groups. It may appear to be too simple to define a fall; however, the difference in definitions can confuse different groups when interpreting information in this research field. The world health organization (WHO) defines a fall as an event that causes a person to accidentally land on the ground or floor or other lower levels [1]. In this definition, the fall's accidental nature is essential, and it excludes intentional landings [1]. While the elderly usually associate the fall with a loss of balance, health care providers define it as a possible injury outcome [2]. The difference in definition also affects the reported statistics in traffic accidents [3], i.e., the Swedish Transport Administration, Trafikverket, excludes killed or injured pedestrians who are accidentally falling on the ground [3]. In the current project, the definition of WHO was taken into account.

A fall can happen to any demographic group; however, adults older than 65 years old are at a higher risk of sustaining an injury as a result of a fall [1], [4], [5]. A previous study suggests that about one-third of adults in their 60th are falling every year, and the risk rises as they get older [6]. A fall injury can cause fracture or laceration in different body segments but usually, forward and backward falls lead to wrist and upper extremity injuries, while sideways falls lead to hip fractures [7]. Figure 1.1 shortly summarizes the fall-induced injuries with their frequency and severity. Among fall-induced injuries, hip fractures are more severe among the elderly since it causes loss of mobility, higher mortality rate, and social and economic costs [8], [9]. Old female adults have a higher risk of hip fracture due to age-related bone loss and falling frequency [10]–[12]. The population demographic is changing in developed countries, and the number of adults reaching older ages increases, which adversely means higher fall incidents and financial and social costs for societies [1], [5]. Furthermore, the fall rate and the risk of injury discourage the elderly from an activity that could worsen their mobility and health conditions [1].

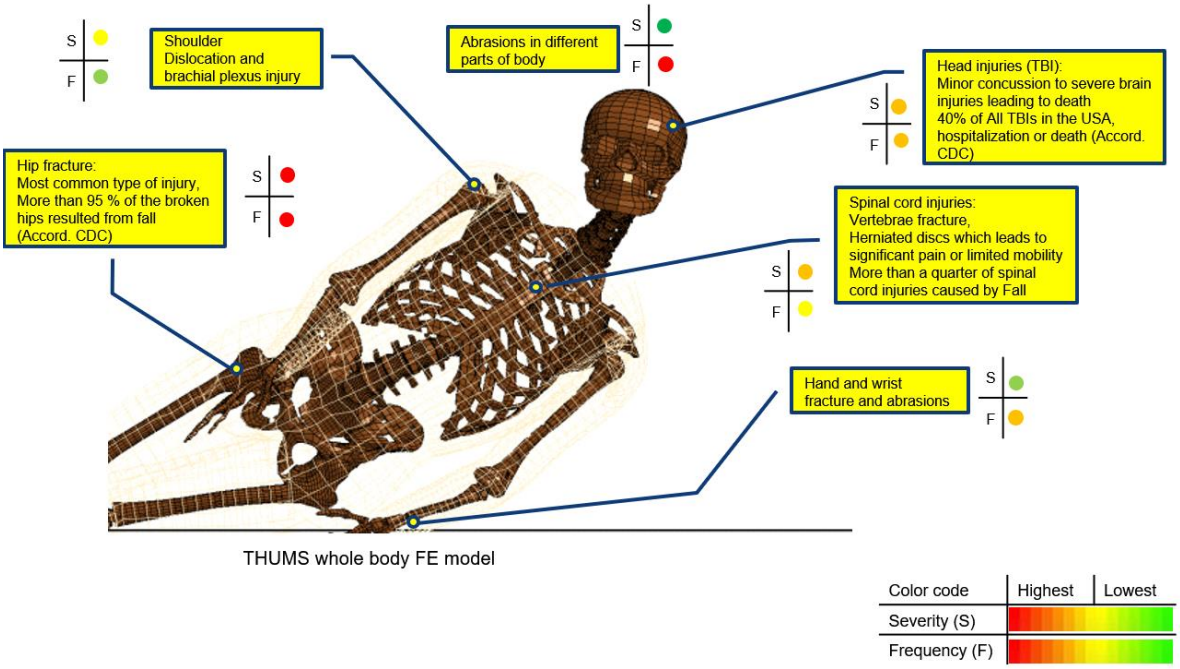

Figure 1.1. summary of possible fall-induced injuries according to previous studies [7], [13].

According to the Swedish transport administration, pedestrians falling outdoors and cyclists account for about 70 percent of the severe injuries in road traffic environments [3]. Another study on traffic fatality in 31 major cities globally suggests that pedestrians and cyclists consist of half of the fatalities [14]. Despite the improvements in traffic accident prevention during past decades [15], cyclists and pedestrians, or more broadly vulnerable road users (VRU), received less attention [14]. Cyclists can enjoy better protection by wearing helmets [16], [17]; however, there is no specific protection for pedestrians. A common element in VRU traffic accidents is the pavements. It appears that a change in the design and construction of the pavements can potentially benefit all VRUs if it can successfully reduce the risk of injury for the elderly females, the most vulnerable demographic group [18], [19]. Another possible protective solution against fall-induced injury is the wearable or inflatable hip protector [20]–[22]. Although the hip protectors were shown to be a beneficial protective tool [22], they can only reduce the risk of injury for an individual user. Contrary to the hip protectors, a compliant pavement potentially reduces the risk of injury for all road users regardless of their demographic group.

The finite element method is a numerical method that could be used to evaluate the potential capability of a proposed solution for reducing the risk of injury. This method is widely used for traffic accident reconstructions and various accidents [23]–[28]. It included several forms of accidents, such as single-vehicle accidents and vehicle-pedestrian accidents, but not fall accidents. Different body segments are also included in the FE models, from a single segment simulation such as human head models [29]–[33] to complete human body models (HBM) such as the total human model for safety (THUMS, Figure 1.2) [24], [25], [27] and the Global Human Body Models Consortium (GHBMC, Figure 1.2) [28], [34], [35].

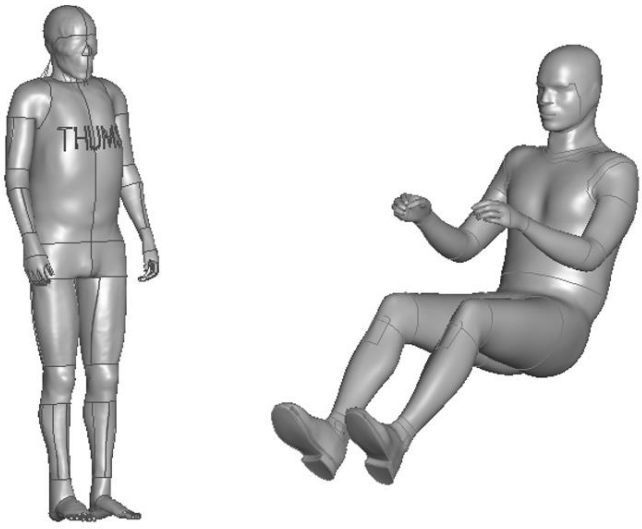

Figure 1.2. A pedestrian THUMS whole-body model ([25], left) and a car occupant GHBMC model ([36], right).

The geometry and mechanical properties of the HBMs were initially developed according to a 50th percentile healthy man [25], [35], and later a family of models was developed to represent the broader range of sexes and ages [27], [28]. The aim of the models was to simulate common car accidents involving car occupants or pedestrians [37], and their capability for simulation of fall-induced injuries has not been thoroughly studied yet. Two critical parameters are different in a fall incident compared to other traffic accidents. A different age population should be studied in the fall incidents [3], and the body configuration during a fall incident is different from a pedestrian or car occupant accident. A recent study [37] used an experimental fall simulator to mimic the sideways falls. The whole body was replaced with effective masses, except for the pelvis and proximal femur section, in which a surrogate pelvis and femur were used [37]. The soft tissue is also replaced with ballistic gelatin [37]. Later, they developed explicit subject-specific finite element models to simulate the same experiments [37]–[39]. Apart from these earlier attempts, which were not complete HBMs, there is no study on fall-induced injuries using the THUMS whole-body model.

The issues with the current state of the art fall biomechanics research motivated the current doctoral thesis. Two main questions were asked in the definition of each study within the project:

- How do different parameters such as age influence the fall injury biomechanics?
- Does the proposed idea of a compliant pavement reduce the risk of major fall injuries, i.e., hip fracture and head injury?

The first question was addressed in papers A, B, and C, and the second question was addressed in papers D and E.

2 Objectives

The thesis's main objective was to better understand the fall-induced injury biomechanics using the THUMS whole-body model and evaluate the rubberized asphalt pavements' capacity to reduce the risk of head injuries and hip fractures.

The first aspect of the project was covered within the first three studies. The specific aim of each study was as follows:

Paper A — To evaluate the effect of body configuration, the trunk angle (the angle between the trunk and vertical), and the pelvis angle (anterior and posterior rotation of the pelvis) on the internal forces induced on the femoral head during sideways falls on the hip.

Paper B — To investigate the effect of soft tissue material modeling on the external and internal forces applied to the femur during sideways falls using the objective CORrelation and Analysis (CORA) method.

Paper C — To study the separate and combined effects of geometrical and mechanical properties changes due to aging on femoral strength.

The second aspect of the project was examined through the following studies. It was hypothesized that a more compliant asphalt mixture could potentially reduce the risk of injury. The aim of the designed studies was as follows:

Paper D — To assess the effect of varying rubber content in the rubberized asphalt samples to reduce the head injury risk in a bicycle and a pedestrian accident reconstruction model.

Paper E — To evaluate the rubberized asphalt mixture's capability to reduce the risk of sideways fall-induced hip fractures.

3 Background

The majority of hip fractures happen because of a fall [7], [40]. A previous study [41] suggested four conditions for a fall that leads to a hip fracture: (i) The fall occurs close to the pelvis segment, (ii) the fall cannot be responded to promptly, (iii) the soft tissue cannot absorb enough energy, and (iv) the remaining energy surpasses the proximal femur strength [41].

In this chapter, a literature review of the main aspects of the thesis was conducted to summarize the previous efforts. The first aspect was understanding the fall biomechanics, where a brief description of the body configuration, pelvis segment, and the aging effects on the femoral strength was presented. Another aspect of the thesis was to examine the compliant asphalt mixture's effectiveness as a preventive tool to reduce fall-induced injuries.

3.1 Body Configuration

Body configuration can significantly affect the outcome of a fall [7], [40], [42]–[47]. An observational study on elderly people suggests that incorrect shifting of weight and stumble are the most common causes of falls in elderly houses (Figure 3.1, [48]). A case-control analysis of a cohort study on community living older females (+65 years old) found the group with hip fractures were mainly fallen sideways, near the hip region [7]. Another study among 206 patients and 100 controls discovered that the majority of the patients had fallen directly to the side [40]. In both studies, the patients could not break their fall with their arm or hand, and an impact on the greater trochanter of the proximal femur occurred. Similar findings were reported in two experimental studies. An experimental study on six young adults examined the body configuration and velocities during a voluntary sideways fall from standing height [42]. They found that only two subjects could break their fall with their hand or arm, and the others directly impacted their hip. Another experimental study on 44 young individuals (19 to 26 years, 31 female) found that 90 percent of the subjects impacted the pelvis. Contrary to the previous study, they found that most subjects impacted their hands and knees prior to the hip impacts [43]. They suggested that the experiment's design, prior knowledge of the fall, such as the floor's compliance, and self-initiation of the fall, can cause these discrepancies among the published results [43].

Figure 3.1. Incorrect weight shifting during walking forward, which led to a sideways fall (Top row), Stumbled while walking, resulting in a backward fall (Bottom row) [48],(License acquired through Copyright Clearance Center).

Previous studies on fall kinematics suggested three body angles to be relevant in the magnitude of the impact forces as a result of a sideways falling (Figure 3.2) [42], [43], [49]. The knee flexion angle was found to be, on average, 109 degrees [42], [49]. The trunk angle, which is the angle between the trunk and the vertical, was measured to be 17.3 degrees (SD = 11.5°) in an experimental fall study [42]. The same study found that a fall with an active muscle could increase the average trunk angle from 13.6 degrees (SD = 11.2°) to 21.8 degrees (SD = 10.4°). Another study on a larger cohort suggests an average trunk angle of 42 degrees when the hip impacts the ground after an initial hand or knee impact [43]. The last body angle is the anterior or posterior rotation of the pelvis (pelvis angle). A recent study explored the effect of variation of the pelvis angle on the generated internal forces measured on the femoral head using a hip impactor simulator [50]. It was found that a 10-degree anterior rotation of the pelvis can lead to the highest internal forces [50]. The experimental study on 44 young subjects found that the average pelvis angle is 8 degrees (SD= 15) posterior rotation.

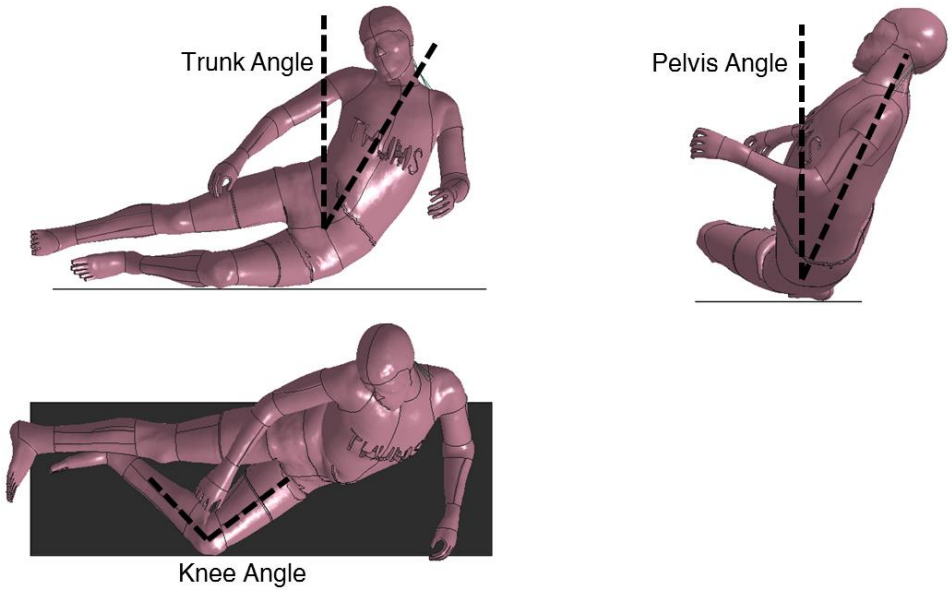

Figure 3.2. Different relevant body angles in a sideways fall incident

Finally, the hip velocity during sideways falls was reported on average 3.0 m/s [46]. The two experiments on young human volunteers reported similar range of falling velocities of 3.17 m/s (SD = 0.47) [42] and 3.01 m/s (SD = 0.83) [43].

3.2 Pelvis Segment

The human body's pelvis segment can be divided into three main sections, as shown in Figure 3.3: Internal soft tissues (Figure 3.3, a, b), external soft tissues (Figure 3.3, c), and bony tissues (Figure 3.4). The internal soft tissue consists of the soft tissues that are medial to the femur, such as the pubic symphysis, ligaments, and cartilages. The bony tissue consists of the femur and pelvis (Figure 3.4). Finally, the external soft tissue consists of the muscular tissue covering the proximal femur, fat, and skin [51], [52].

(a)

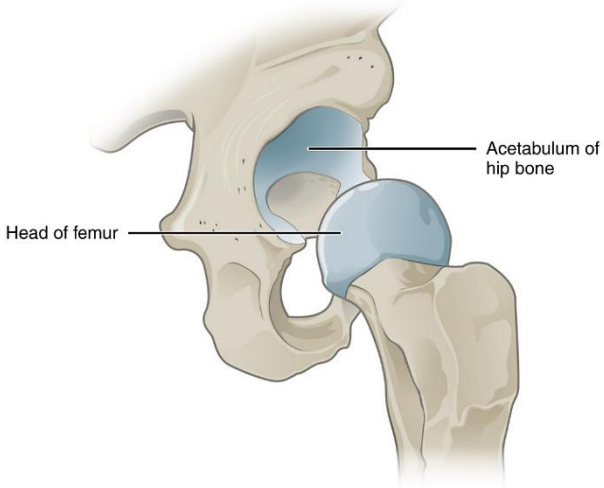

(b)

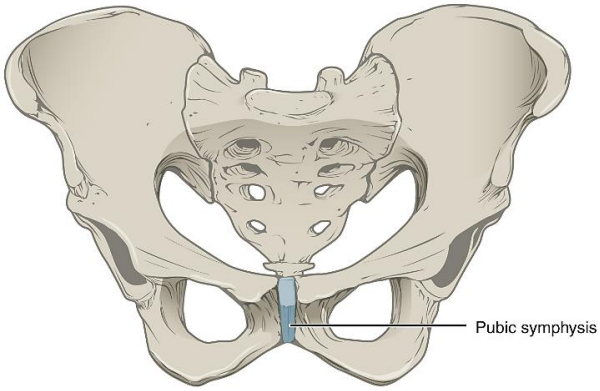

(c)

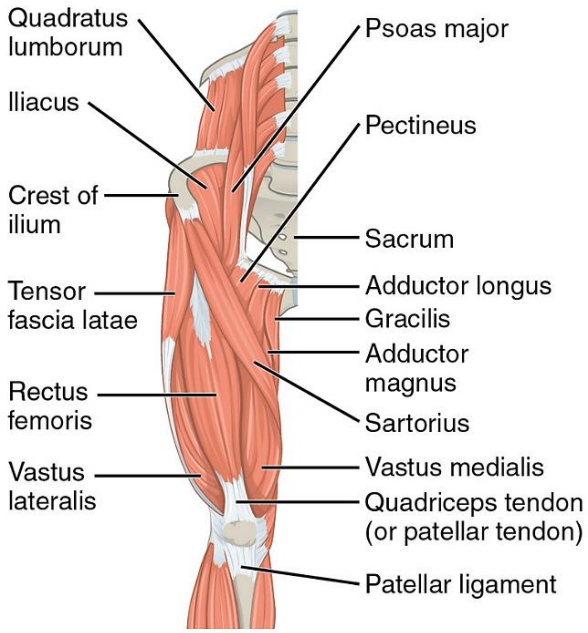

Figure 3.3. Internal soft tissues (cartilaginous joints), (a) acetabulum and (b) pubic symphysis, and (c) external soft tissues excluding skin and fat tissue, [53] (CC BY 4.0, Download for free at http://cnx.org/contents/14fb4ad7-39a1-4eee-ab6e-3ef2482e3e22@11.1.)

The pubic symphysis is a cartilage tissue between the left and right pubic bone (Figure 3.3, b). The femoral head and the acetabulum form a ball and socket joint named the hip joint (Figure 3.3, a). There are articular cartilage and several ligaments responsible for increasing the hip joint's stability [51]. The proximal femur has three important geometric features: the femoral head attached to the acetabulum, the femoral neck, the region between the femoral head and femoral shaft, and the greater trochanter, which is located on the lateral and proximal side of the femur (Figure 3.4). The muscular tissue covers the greater trochanteric area of the proximal femur. A layer of fat and a thin layer of skin covers the muscles and bones and surrounds the pelvis segment.

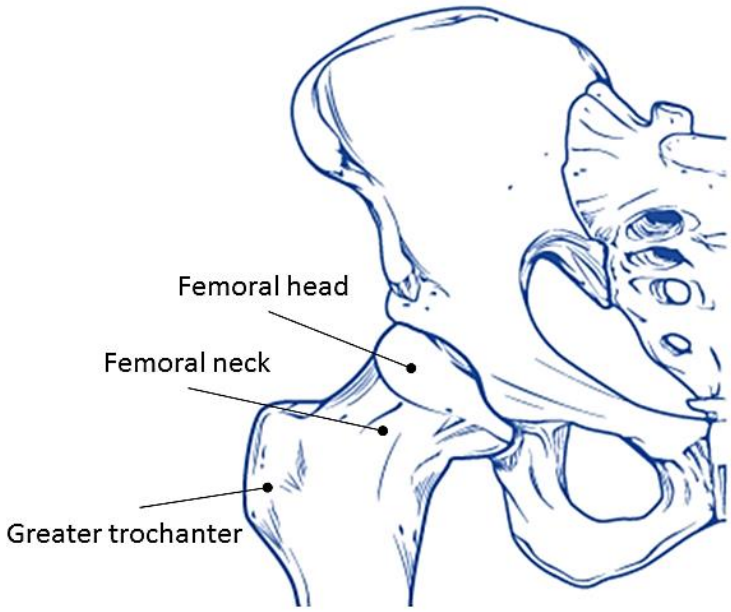

Figure 3.4. Geometrical features of the proximal femur, [53] (CC BY 4.0, Download for free at http://cnx.org/contents/14fb4ad7-39a1-4eee-ab6e-3ef2482e3e22@11.1.)

In any impact to the side of the hip region, the external and internal soft tissues participate in the force attenuation [54]–[56], and the bony tissue carries the rest of the impact forces [56], [57]. Thus, the soft tissue force attenuation capacity and the femoral strength are the key parameters in the fall outcome.

3.2.1 Soft tissue

Soft tissues in the pelvis segment are the natural shock-absorbing elements that can reduce the impact forces [56], [58]–[61]. Previous studies on fall injury found that soft tissue thickness plays an important role in force attenuation (Figure 3.5) [56], [59], [62]. A previous study on 21 postmenopausal females and 42 age-matched controls revealed that a lower soft tissue thickness was associated with a higher risk of hip fracture [62]. Another study conducted on the femur surrogate and different soft tissue thicknesses indicated a 70 N decrease of internal forces measured on the femoral head for every 1 mm increase in the thickness [56]. Another numerical study proposed a power-law relationship between the thickness and the impact force [59]. The soft tissue thickness measures in different previous studies reveal that the average thickness across different study populations is 32 mm (SD = 23.2), and the average for a group with hip fracture reduces to 28.3 mm [63].

In addition to the soft tissue thickness, the local stiffness of the soft tissue could play an essential role in the force attenuation capacity during a sideways fall [20], [55], [60], [63]. An indentation test on 15 elderly females has been measured the soft tissue stiffness in 9 locations around the greater trochanteric area [20]. The soft tissue directly over the greater trochanteric area was the stiffest (34.4 kN/m), and the least measured stiffness was 14.1 kN/m [20]. Muscle activation can affect the overlaying soft tissue's energy absorption capacity by increasing stiffness [20]. A previous study on a mechanical hip impact simulator suggested a hip abductor muscle activation could substantially reduce the femoral neck's stresses during a sideways fall [55].

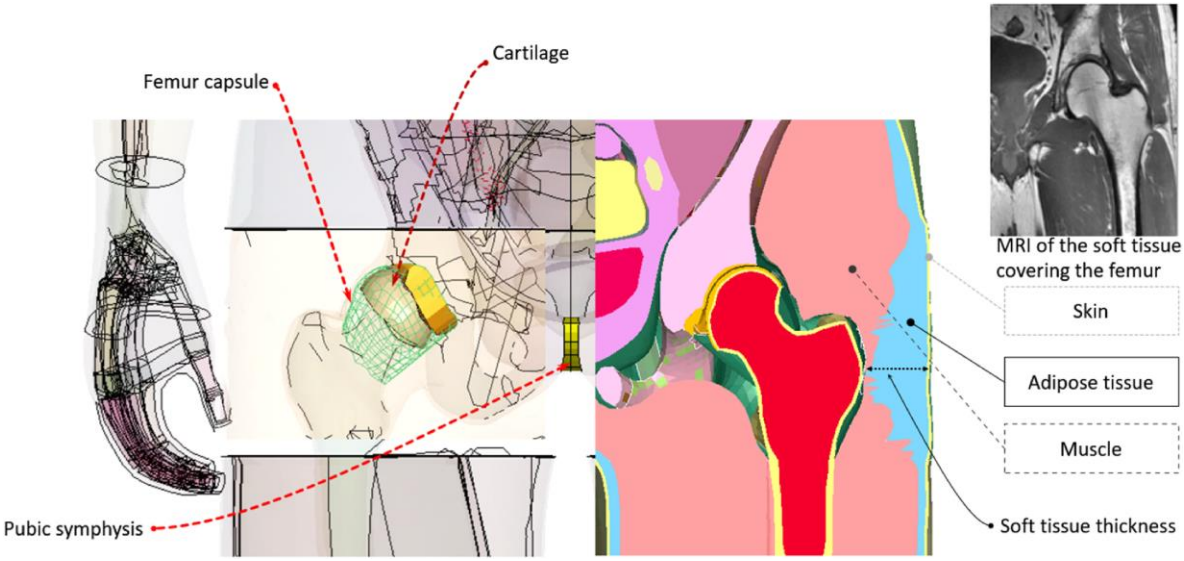

Figure 3.5. Modeled soft tissue distribution [54] of the adipose and muscle tissues over the greater trochanter using the MRI data (CC BY 4.0, The MRI image [64] has the following license agreement: CC BY-NC 3.0).

Previous studies proposed different material properties for the adipose tissue [65]–[71], muscle [65], [66], [72]–[79], skin [79], cartilage [80], pubic symphysis [81], [82], and acetabular ligaments [83], [84] (Table 3.1). The proposed models for muscle were mainly nonlinear to capture the large deformations of the tissue during a sideways fall [85].

Table 3.1. Literature review of constitutive models and material properties for various soft tissues [54]

Soft tissue	**Material Model**	**Material parameters**	**From Study**
Skin[#]	Mooney-Rivlin	ρ = 1.133 g/cm^3, C_{10} = 0.0094 MPa, C_{01} = 0.0 MPa, C_{11} = 0.082 MPa, ν = 0.499	[79]
Cartilage[*#]	Ogden	ρ = 0.862 g/cm^3, μ = 0.19 MPa, α = 4.99, ν = 0.499	[80]
Pubic symphysis[#]	Mooney-Rivlin	ρ = 1.0 g/cm^3, C_{10} = 0.1 MPa, C_{01} = 0.45 MPa, C_{11} = 0.6 MPa, ν = 0.499, g_1 = 0.0224 MPa, β_1 = 0.7463 1/s, g_2 = 0.3741 MPa, β_2 = 0.031 1/s	[81], [82]
Acetabular ligament[*#]	Ogden	ρ = 1.0 g/cm^3, μ = 0.0335 MPa, α = 58.70, ν = 0.499	[83], [84]
Adipose tissue models			
Al-Dirini[#]	Ogden	ρ = 0.92 g/cm3, μ = 0.001165 MPa, α = 16.2, ν = 0.499	[65]

Brosh[#]	Mooney-Rivlin	ρ = 0.92 g/cm3, C10 = 1.595e-2 MPa, ν = 0.499	[71], [73]
Comley[#]	Ogden	ρ = 0.92 g/cm3, μ = 0.0017 MPa, α = 23, ν = 0.499	[70]
Engelbrektsson[#]	Ogden	ρ = 0.92 g/cm3, μ = 3e-5 MPa, α = 20, ν = 0.49, g1 = 3e-3 MPa, β1 = 310 1/s	[67]
Krouskop[#]	Ogden	ρ = 0.92 g/cm3, μ = 0.00399 MPa, α = 8.82, ν = 0.499	[68]
Omidi[#]	Ogden	ρ = 0.92 g/cm3, μ = 3.4e-4 MPa, α = 3.89, ν = 0.499	[69]
Then[#]	Ogden	ρ = 0.92 g/cm3, μ1 = -2.2e-2 MPa, α1= -0.11, μ2 = -4.04e-9 MPa, α2 = -31.9, ν = 0.495	[66]
Muscle models			
Al-Dirini[#]	Ogden	ρ = 1.133 g/cm^3, μ = 1.907e-3 MPa, α = 4.6, ν = 0.49, g_1 = 5.339e-3 MPa, β_1 = 0.1666 1/s	[65]
Hedenstiena[#]	Ogden	ρ = 1.133 g/cm^3, μ = 1.3337e-2 MPa, α = 14.5, ν = 0.49, g_1 = 0.522 MPa, β_1 = 1020 1/s, g_2 = 3.211e-3 MPa, β_2 = 400 1/s, g_3 = 3.375e-3 MPa, β_3 = 65 1/s, g_4 = 3.29e-3 MPa, β_4 = 30 1/s, g_5 = 3.8e-3 MPa, β_5 = 0.1 1/s	[72]
Linder-Ganz[#]	Mooney-Rivlin	ρ = 1.133 g/cm^3, C_{10} = 4.25e-3 MPa, ν = 0.499	[73]
Takaza[**]	Ogden	ρ = 1.133 g/cm^3, μ = 1.685e-3 MPa, α = 15.4, ν = 0.499, g_1 = 7.15e-2 MPa, β_1 = 6666.67 1/s, g_2 = 2.49 MPa, β_2 = 6.666e5 1/s, g_3 = 2.77e-1 MPa, β_3 = 6.6667e13 1/s	[75]
Then[#]	Ogden	ρ = 1.133 g/cm^3, μ_1 = 1.558e-3 MPa, α_1= 1.316, μ_2 = -1.582e-8 MPa, α_2 = -18.36, ν = 0.495, g = 5.34e-3 MPa, β = 0.1667 1/s	[66]
Van Loocke Ogden[*]	Ogden	ρ = 1.133 g/cm^3, μ = 1.367e-4 MPa, α = 8.805, ν = 0.499, g_1 = 1.217e-3 MPa, β_1 = 1.667 1/s, g_2 = 3.126e-4 MPa, β_2 = 0.1667 1/s, g_3 = 6.773e-5 MPa, β_3 = 3.33e-2 1/s, g_4 = 2.605e-4 MPa, β_4 = 1.667e-2 1/s, g_5 = 1.458e-4 MPa, β_5 = 3.3e-3 1/s	[76], [77]
Van Loocke QLV[**]	QLV	ρ = 1.133 g/cm^3, g_1 = 3.96e-4 MPa, β_1 = 1.6667 1/s, g_2 = 1.018e-4 MPa, β_2 = 0.16667 1/s, g_3 = 2.205e-5 MPa, β_3 = 3.33e-2 1/s, g_4 = 8.482e-5 MPa, β_4 = 1.67e-2 1/s, g_5 = 4.75e-5 MPa, β_5 = 3.3e-3 1/s, c_1 = 1.293e-3 MPa, c_2 = 9.11e-4 MPa, c_3 = 1.087e-2 MPa	[76], [77]
Zheng[*#]	Ogden	ρ = 1.133 g/cm^3, μ = 3.044e-3 MPa, α = 6.5, ν = 0.49, g_1 = 1.218e-2 MPa, β_1 = 0.1667	[78]

[*] Material parameters were fitted with the Ogden model using MATLAB V2019 according to the experimental results of the references.

[**] The material models were developed according to experiments on Porcine tissues.

[#] The material models were developed according to experiments on human tissue.

3.2.2 Bone tissue

After attenuation of the impact force by the soft tissue, the remaining are applied to the femur, which needs to resist it by its strength. The femur consists of cortical and trabecular bones, and each of the bone types contributes to the femoral strength [86], [87]. There is a great deal of debate surrounding the contribution of the cortical and trabecular bone. Depending on the location of impact on the proximal femur, loading condition, and age of the subjects, the cortical bone contribution can vary between 90 to 60 percent [86]–[89].

The cortical and trabecular bones have been modeled differently in different studies. It has been shown that the cortical bone has transverse isotropic mechanical properties [90]–[96], especially at the apparent level (Figure 3.6). The transverse direction is perpendicular to the shaft axis, and the longitudinal direction is along the direction of osteons [92]. The ultimate or failure strains are also

asymmetric for the cortical bones [92], in which the strength of the cortical bone is higher in compression compared to tension.

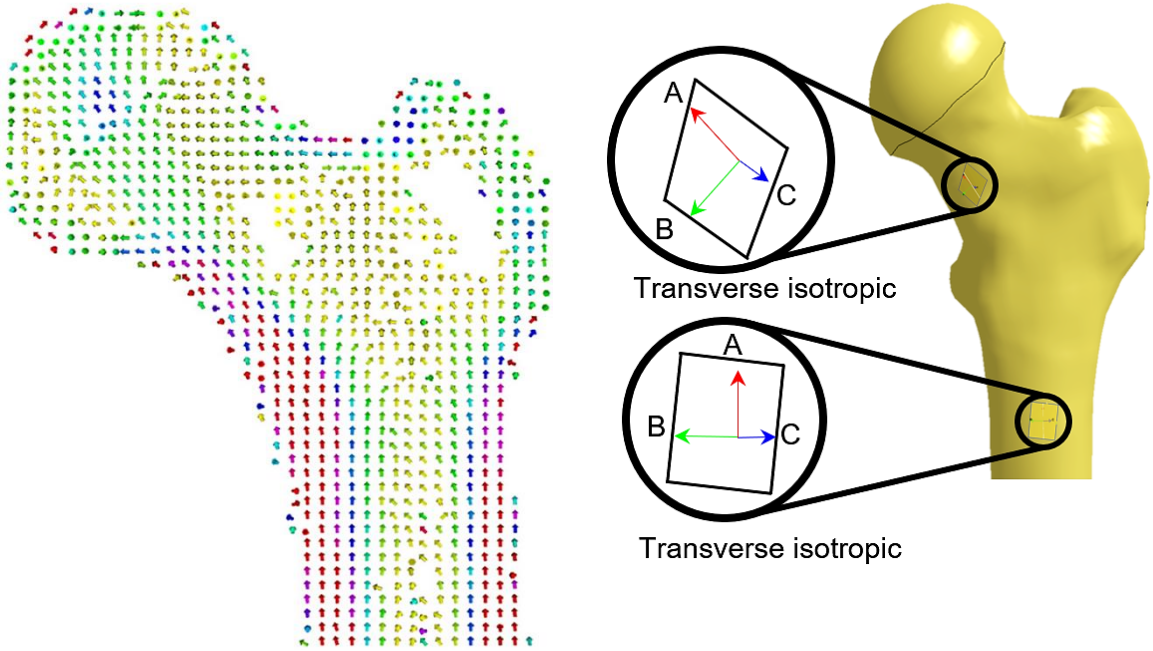

Figure 3.6. (Left) The proximal femur's principal stiffness orientation was measured using the High Resolution-peripheral Quantitative Computed Tomography (HR-pQCT, colors represent the stiffness value: the highest represented 4 GPa (Red), and the lowest value represented 1 MPa (Yellow)) [96] (License acquired through Copyright Clearance Center); (Right) The proximal femur was modeled using a transverse isotropic material model for the femoral shaft and neck, where the green and blue arrows (B and C) represented the transverse plane [97] (CC BY 4.0).

Several studies assessed the proximal femur's strength using a similar experimental setup [98]–[100]. The femur's proximal section is positioned in a relevant sideways fall; the shaft is rotated 10° with respect to horizontal, and the neck is internally rotated to 15° [98], [99]. The experiments were performed with different displacement rates. However, the displacement rate of 100 mm/s is a better representative of a sideways fall on the hip [98]. According to previous studies, several parameters affect the strength of the proximal femur, such as age, sex, bone mineral density (BMD), displacement rate, and geometrical characteristics of the proximal femur [99], [101]–[104]. A recent study summarized the relevant experimental studies on the strength of the proximal femur. The femur's average strength was 4586 N and 2872 N for elderly males and elderly females, respectively [100].

3.2.3 Aging effect

The most vulnerable age group in fall-induced injuries is the older adults; consequently, it is essential to review the effect of aging on femoral strength and soft tissue material properties. In addition to tissue-level changes to the bone and soft tissue, older adults may suffer from lower balance, stiffer and inadequate posture control, impaired ability to avoid a fall after a disturbance, and vision impairment [4]. The focus of this literature review is on the tissue level changes due to aging.

The femoral strength decreases as age advances. An experimental study on eight older adults (mean age of 74 years) and nine younger individuals (mean age of 33 years) suggested about 3500 N lower femoral strength for the older adults [105]. The changes in the femoral strength are sex-dependent as well. A recent study in a larger cohort of 100 cadaveric femurs suggests the femoral strength reduces by about 640 N and 860 N per decade for males and females [106]. Two parameters change with age, geometrical characteristics of the proximal femur and the mechanical properties of the cortical and trabecular bones [92], [101], [107]–[110]. A recent study has concluded that the BMD, sex, and age are enough to clinically evaluate femoral strength. Moreover, the loading rate and neck-shaft angle are not increasing the accuracy of predictions [111].

It is shown that the average cortical thickness, cortical cross-sectional area, and moment of inertia are negatively associated with age [112]. The sex differences are noticeable in both the size of the femur (neck width) and the changes in the neck geometry due to aging [113], [114]. In several detailed studies, it was shown that the cortical thickness changes in each quadrant of the femoral neck are dissimilar (Figure 3.7) [107], [108], [115]–[118]. A five-year longitudinal study suggested that the average cortical thickness in the superior section of the femoral neck gets thinner at a faster rate than in the inferior section, and males experience slower changes than females [107], [112], [115], [117], [119].

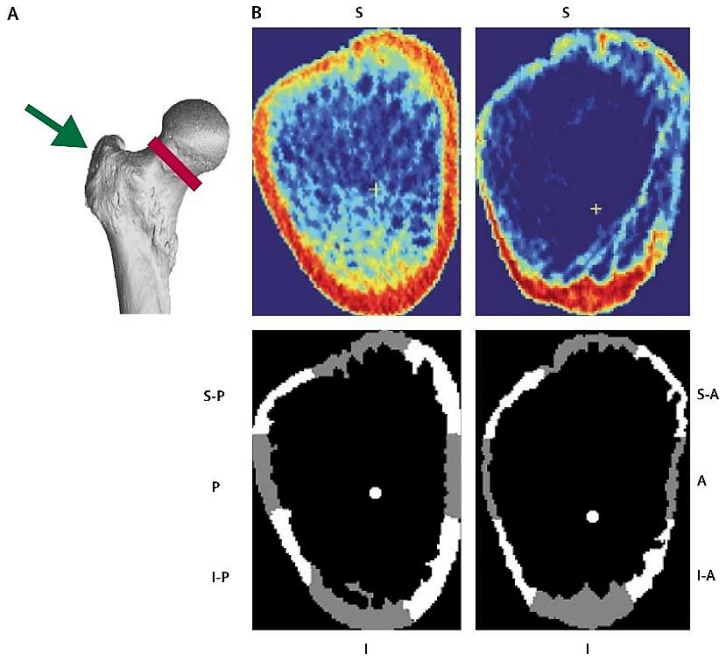

Figure 3.7. A cross-sectional QCT image of the femoral neck of an old female (80 years old, right) and a young subject (20 years old, left) where the cortical thickness and mineral density decayed for the old female [108]. The cortical thickness changes are not equal in different quadrants, and it decreases faster in the superoanterior (S-A) quadrants than in the superoposterior (S-P), Inferoposterior (I-P), and Inferoanterior (I-A) due to aging (S-A>S-P>I-P>I-A) [117] (License acquired through Copyright Clearance Center).

The cortical and trabecular bones experience similar mechanical properties changes in males and females [102], [120], [121]. The Young's and shear modulus of the cortical bone reduces 3 and 4 percent per decade of age for the cortical bone, while the ultimate strain decreases about 5 to 10 percent of its initial value per decade. The yield strains considered to be independent of the age [33], [91], [92], [120]–[123]. The changes in the cortical bone transit a ductile bone to a more brittle one

[109]. A similar change happens for the trabecular bone. The modulus decreases approximately by 5 percent per decade[122], [124].

The soft tissue is also affected by aging [125]. A previous study on the compressive stiffness and damping properties of the soft tissue using the dynamic indentation method revealed the stiffness and damping were 2.9 and 3.5 times smaller in older females (+65) compared to the younger females (19-30) [125]. It was also indicated that the two parameters were not associated with the soft tissue thickness [125]. The changes can reduce the force attenuation capacity of the soft tissue for the elderly.

3.3 Preventive Tools

Understanding the mechanism of injury, fall dynamics, and the target population group can help develop preventive tools and precautionary measures. Several preventive measures are intended to prevent the fall in the first place, such as fixing narrow steps or slippery rugs at home or using walkers [1]. Even with these measures, elderly adults will fall due to physical frailty [1]. Consequently, the next preventive measures should be focused on reducing the impact forces or increasing the older adults' femoral strength. The concept of active aging is introduced by WHO to improve older adults' health conditions [1]. Reducing the impact forces can be done with different techniques[126]–[129]. In this section, the preventive tools to reduce the impact forces are reviewed.

Wearable or inflatable hip protectors (Figure 3.8) can attenuate the impact forces and reduce them below the strength limit of the proximal femur [22], [130], [131]. The hip protectors either dissipate energy or change the loading location to a less vulnerable location [22], [132]. Despite the hip protectors' promising ability, there are still conflicting results regarding the hip protectors' clinical effectiveness [130], [133]. It is the responsibility of the user to put on the hip protector in a proper manner. A study on three soft shell hip protectors available in the market revealed that a displaced hip protector (from the intended position) could increase the femoral neck's peak forces up to 60 percent compared to the correctly positioned hip protector [133].

(a)

(b)

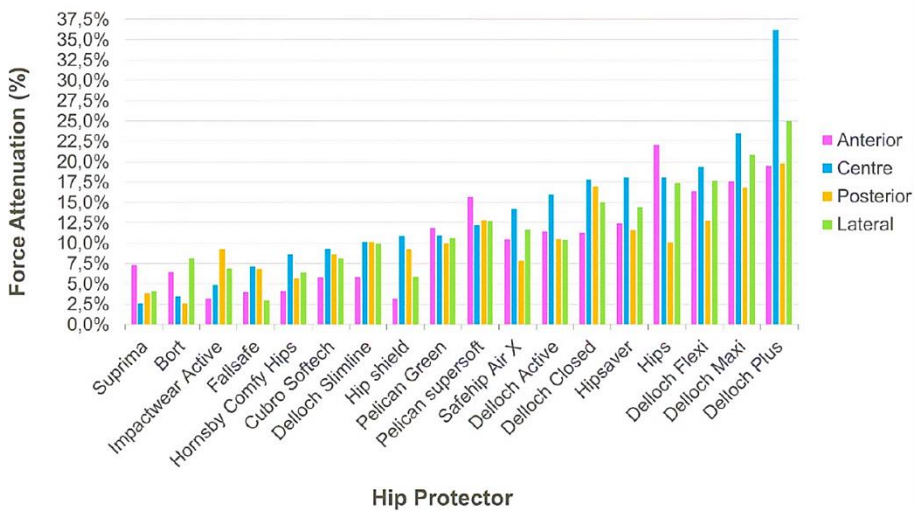

Figure 3.8. (a) Typical wearable hip protectors that are available in the market [134] and their corresponding force attenuation (b) in different situations in which they were positioned correctly over the greater trochanter (center) and when they were misplaced in a different position [134]. (License acquired through Copyright Clearance Center).

Another tool to attenuate the impact forces is shock-absorbing floors (Figure 3.9). Unlike hip protectors, the compliant floorings are not sensitive to the users and the correct placement. Moreover, hip protectors can only protect one individual, which might not be the case in elderly houses. The primary condition for the shock-absorbing floors other than their force attenuation properties is locomotion and mobility. The softer floors could improve the force attenuation, but it adversely affects the stability and balance and could cause more falls. Several intervention studies were carried out in the elderly houses to assess the indoor shock-absorbing floors [135]–[138]. Results in the effectiveness of the shock-absorbing floor suffer from a similar issue, like the wearable hip protectors. While some studies suggest that the shock-absorbing floor can effectively reduce the risk of serious fall injuries [135], [137], a more recent study found no significant effect on preventing serious fall-induced injuries [139].

(a)

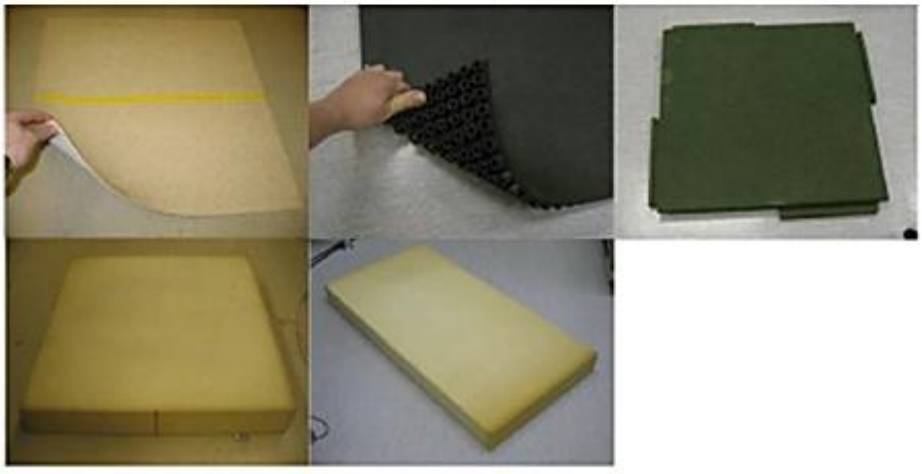

(b)

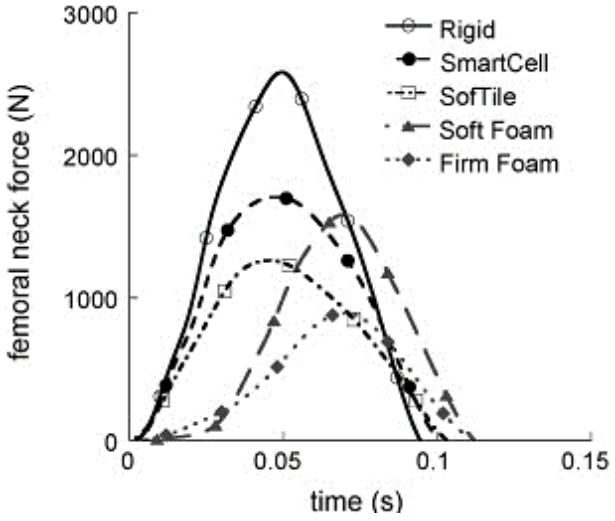

Figure 3.9. Typical shock-absorbing floorings(clockwise from top): Rigid, SmartCell, SofTile, Firm Foam, Soft Foam (a) [136], and their corresponding femoral neck forces, evaluated using a hip impact simulator (b) [136] (License acquired through Copyright Clearance Center).

Older adults reduce their outdoor activities, partly due to the fear of falling. In addition to older adults, pedestrians from other demographics are also at risk of falling outdoors. A beneficial measure to reduce the risk of injury for pedestrians could be compliant shock-absorbing pavements. Only a few studies investigated the effect of reducing the stiffness of the asphalt mixtures (Figure 3.10) on reducing head injury risk [129], [140]. A previous study on several asphalt mixtures suggests a 45% reduction in skull fracture risk in an asphalt mixture containing 60%vol. rubber [140].

Figure 3.10. Rubber asphalt mixture (left), rubber concrete casting (right) [140] (License acquired through Copyright Clearance Center).

4 Method

In this section, a summary of the methods used in the project is presented. Initially, the numerical method and the execution methods were introduced. Then, the whole-body model, THUMS, and the required enhancement in the hip region are presented, and the force evaluation references for internal and external forces are established. Section 4.3 introduces the bone damage model, which was intended to make the bone both transverse isotropic and asymmetric regarding the failure properties. Later, the hyperelastic mechanical properties formulations, which were implemented in the soft tissue study, are presented. Section 4.4 discusses the experimental and modeling of rubberized asphalt mixtures and the material modeling validation method.

4.1 Nonlinear and Dynamic Finite Element Analysis

There are three types of solutions to solve complex biomechanical questions: experimental, analytical, and numerical solutions. Experiments are time-consuming, demanding, and expensive solutions which are usually limited in the initial and boundary conditions. Analytical methods can provide the exact solution to the problem. However, it becomes difficult to find a solution for complex questions. On the other hand, numerical methods can solve complex questions, and they provide more flexibility in testing different initial and boundary conditions. Moreover, the study of fall biomechanics involves the studies of injury cases that could not be reproduced in a controlled experimental setup with human subjects. Therefore, numerical methods can be employed to solve the complex questions of fall biomechanics.

Two types of analysis can be used in the Finite element method to solve a given computational question: linear analysis and nonlinear analysis. The linear analysis assumes that the deformations are proportional to the loads and infinitesimal, and the stiffness matrix is constant and independent of loading conditions [141]. Linear analysis can simplify the computational process and minimize computational costs and time. Within the assumptions for linear analysis, the displacement vector (U) can be calculated using the finite element static equilibrium (equation 1).

$$L = \boldsymbol{K}U \qquad 1$$

Where **K** is the stiffness matrix, and **L** is the external forces, assuming initial undeformed configuration. On the other hand, the linear analysis cannot be used when any of the following nonlinearities exist in the model where the deformed configuration cannot be approximated to be close to the initial one:

- Geometric nonlinearity includes large deflections and strains, large displacement, and rotations even with small stains

- Material nonlinearity, stress-strain relation is nonlinear
- Nonlinear boundary conditions, changing boundary conditions with time or deformation

Different phenomena can cause the geometrical nonlinearity: large strains in which the deformation of the domain is no longer infinitesimal (Grad U<< 1) [142]; large rotation in which a domain only rotates with infinitesimal strains; large displacement with or without rotation which could have infinitesimal strains. In these cases, stress and strains can be described with second Piola-Kirchhoff stress and Green-Lagrange strain [141]. Nonlinearity in the material can occur when the stress-strain relation is nonlinear such as in hyperelastic or elastic-plastic material. When the displacement and strains are infinitesimal, engineering stress and strains can still be used. Finally, when the external loads change with time or deformation, which is a common phenomenon in contacts, the boundary condition is no longer constant. The latter can happen in any other nonlinearities (Figure 4.1).

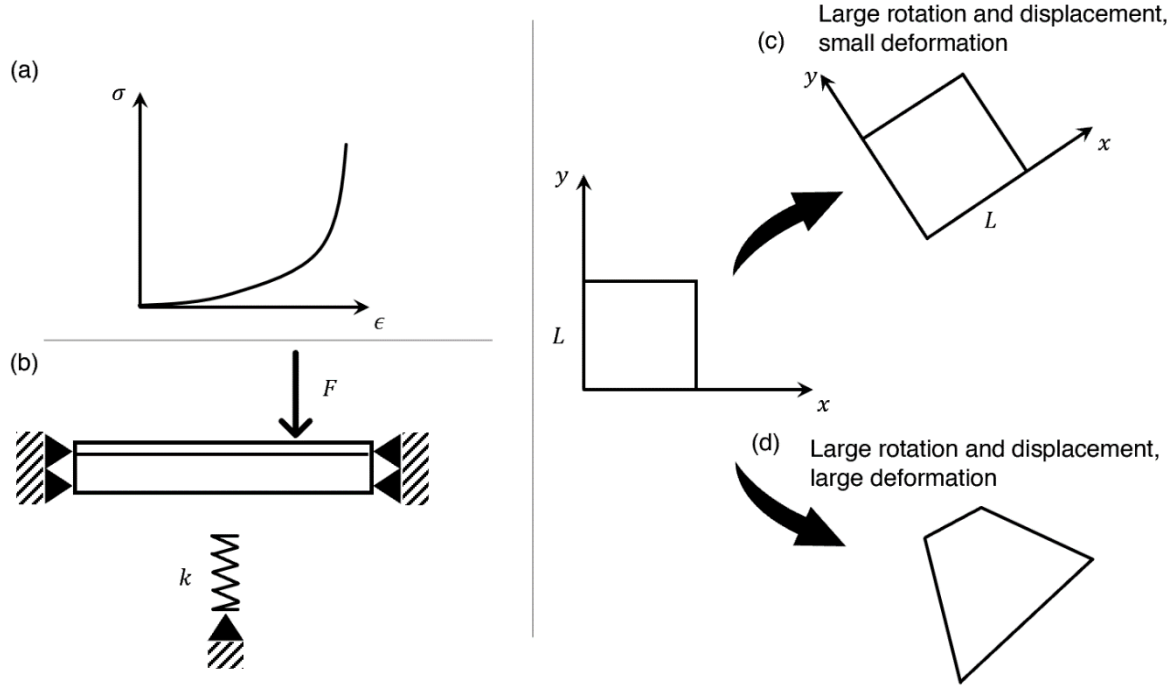

Figure 4.1. (a) material nonlinearity, (b) boundary condition nonlinearity, (c) geometrical nonlinearity, large displacement and rotation, small deformation, (d) geometrical nonlinearity, large displacement and rotation, large deformation.

Although it is possible to solve all problems using nonlinear analysis, the use of linear analysis and infinitesimal strain formulation could be computationally effective and provide an insight into the response. However, the nonlinear analysis is frequently necessary for impact biomechanics due to the nonlinearities in the boundary (contact and changing load), geometry (large deformations of soft tissue under loading), and material (hyperelastic or anisotropic material models for common soft and hard tissues). The finite element equation (equation 1) for nonlinear analysis can be written as:

$$\boldsymbol{L}(U) = \boldsymbol{K}(U)U \qquad 2$$

If the quantities such as displacement and strain are expressed as a function of time and the initial position (Lagrangian approach), the displacement (U) for any node in the domain will be:

$$\boldsymbol{x}(X,t) = X + U(X,t) \quad (3)$$

Where x is the current coordinate of the node and X is the initial coordinates of the same node. The strain can now be defined as the relative motion of two neighboring nodes. First, the deformation gradient (F) needs to be evaluated (equation 4):

$$F = \frac{\partial}{\partial X}(\boldsymbol{X} + \boldsymbol{U}) = \boldsymbol{I} + \frac{\partial \boldsymbol{U}}{\partial X} \quad (4)$$

The Green strain tensor can be evaluated:

$$\epsilon_g = \frac{\mathbf{1}}{\mathbf{2}}(\boldsymbol{F^T}.\boldsymbol{F} - \boldsymbol{I}) \quad (5)$$

The Green strain tensor is symmetric, and rigid body rotations will not affect the accuracy of computations. The Green strain tensor can also be described as the infinitesimal strain term in addition to the quadratic terms [141].

Another aspect of impact biomechanics is the dynamic (transient) loading. Dynamic analysis can be used in cases where the inertia forces are not negligible compared to the applied external loads. Car crash simulations, sideways fall, or shockwave interaction with soft tissue are examples of nonlinear dynamic analysis which could be solved using the time integration of the equation of motion. The equilibrium equation is:

$$\boldsymbol{M}\ddot{u}(t) + \boldsymbol{C}\dot{u}(t) + \boldsymbol{K}u(t) = \boldsymbol{L(t)} \quad (6)$$

Where M is the mass matrix, C is the damping matrix, and L is the external forces. Equation 6 can be written as:

$$\boldsymbol{F_I}(\boldsymbol{t}) + \boldsymbol{F_D}(t) + \boldsymbol{F_E}(t) = \boldsymbol{L(t)} \quad (7)$$

Where the first term denotes inertial forces, and the second and third terms denote damping and internal forces, respectively. Equation 6 can be solved with different integration methods. For instance, the discretized equivalent of the derivatives in equation 6 can be written as follows, using the central difference method:

$$\begin{cases} \ddot{u}(t) = \dfrac{\dot{u}(t+\Delta t) - \dot{u}(t)}{\Delta t} \\ \dot{u}(t+\Delta t) = \dfrac{u(t+\Delta t) - u(t)}{\Delta t};\ \dot{u}(t) = \dfrac{u(t) - u(t-\Delta t)}{\Delta t} \end{cases} \quad (8)$$

Equation 6 can now be solved for *u(t+Δt)* based on the equilibrium in time *t* by replacing equation 8.

$$\left(\boldsymbol{M} + \frac{1}{2}\Delta t\boldsymbol{C}\right)u(t+\Delta t) = \Delta t^2\boldsymbol{L(t)} - (\Delta t^2\boldsymbol{K} - 2\boldsymbol{M})u(t) - (\boldsymbol{M} - \frac{\Delta t}{2}\boldsymbol{C})u(t-\Delta t) \quad (9)$$

In order to maintain the computational stability, the largest time step size (*Δt*) needs to be lower than the 2/(highest natural frequency). Several commercial programs are available for finite

element analysis which can be used to solve the complex equation of motion, and LS-Dyna was used in all studies.

A fall is a dynamic analysis with the effects of mass/inertia and damping. There are two types of dynamic analysis available for this purpose: implicit and explicit. The explicit method was selected for several reasons. The explicit analysis is cheaper concerning computational costs since it avoids several stiffness matrix inversions and directly evaluates the nodal accelerations. The explicit analysis offers a cost-effective computational solution for the nonlinear material models and contacts compared to implicit analysis [143]. Besides the choice between explicit and implicit analysis, it is possible to choose between the shared memory parallel (SMP) processing or the massively parallel (MPP) processing capabilities. The MPP solver can considerably reduce the simulation time compared to SMP. Thus, the MPP solver was used for more complicated simulations such as a whole-body model (papers A, B, E), and the SMP solver was used for simple simulations such as head models or bone simulations (papers C, D). The number of processors in MPP solvers can be optimized since the optimized number of processors is not always equal to the highest number of processors. In most MPP simulations (papers A, B, E), six processors were selected. Finally, the solvers were chosen to be double precision. The simulation time could increase approximately 30 percent compared to single precision; however, it ensures the independence of results from numerical round-offs [143].

4.1.1 THUMS, a Whole-Body Model

The THUMS v4.02 represented a medium-size adult male (50th percentile) with a weight of 76 kg and a height of 177 cm [25]. This version includes the skeletal system, brain, internal organs, and soft tissue (flesh). The original model was developed for pedestrian and car occupant accidents; consequently, it was necessary to revise the model for required enhancements. First, the soft tissues' geometry and constitutive model, both the internal and external ones, were revised to become more representative of those tissues [80], [81], [83], [84], [144]–[148]. In section 4.3, the constitutive material models are presented briefly (paper B). Then, the model was positioned at different trunk and pelvis angles (paper A). The bones were turned rigid during the positioning phase of each fall simulation, and the positioned model (with deformable bones) later was impacted to the rigid ground to evaluate the internal forces generated on the femoral head in each of the body configurations. The proximal femur's geometry and mechanical properties were also revised in Paper C to represent the elderly adults better. The small female model is homogenously scaled down (0.87) from the medium size male model (Figure 4.2).

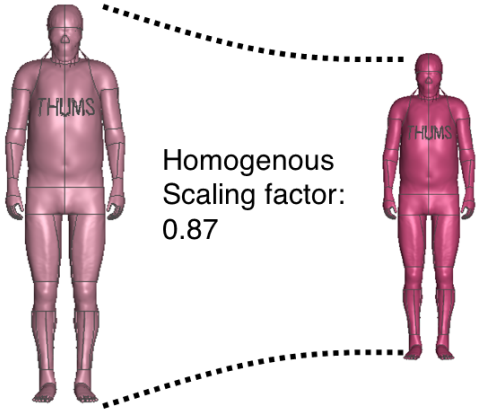

Figure 4.2. Homogenous scaling of the small female model from the medium-size male model.

4.1.2 Force Evaluation in the FE Model

The fall-induced forces can be measured in several locations. Whenever the impact forces in the hip segment model or whole-body models (paper B and E) were evaluated on the lateral side of the soft tissue (impact side), it was denoted as the external forces. In contrast, when the forces were evaluated on the femoral head, which is in contact with the acetabulum, it is denoted as the internal forces (Figure 4.3).

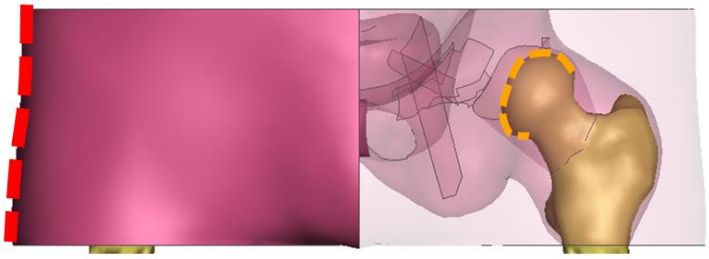

Figure 4.3. The external forces were measured on the impact side (red dished line), and the internal forces were measured on the femoral head (orange dashed line).

4.2 Bone Damage Model

The original material model for cortical bone was isotropic and had similar failure criteria for compression and tension. Moreover, the failed elements were deleted from the calculation. The failure mode in which the corresponding element could be deleted can adversely affect the numerical stability of the model, given the large mesh size of the femur and the whole-body model's complexity. The cortical bone was modeled using a transverse-isotropic model, and the asymmetry of the bone failure was considered using a simplified damage model. There are limited options available for the solid element with non-isotropic material properties in the LS-Dyna. The damage onset was set to the yield strain in each direction. The elements were not deleted after they reached their ultimate strain. Instead, the corresponding stiffness in the same direction was reduced to 1 percent of the initial value (Figure 4.4). This material model could improve the cortical bone's material modeling by including the asymmetry in both stiffnesses and failure criteria and alleviating the original model's mesh integrity issue.

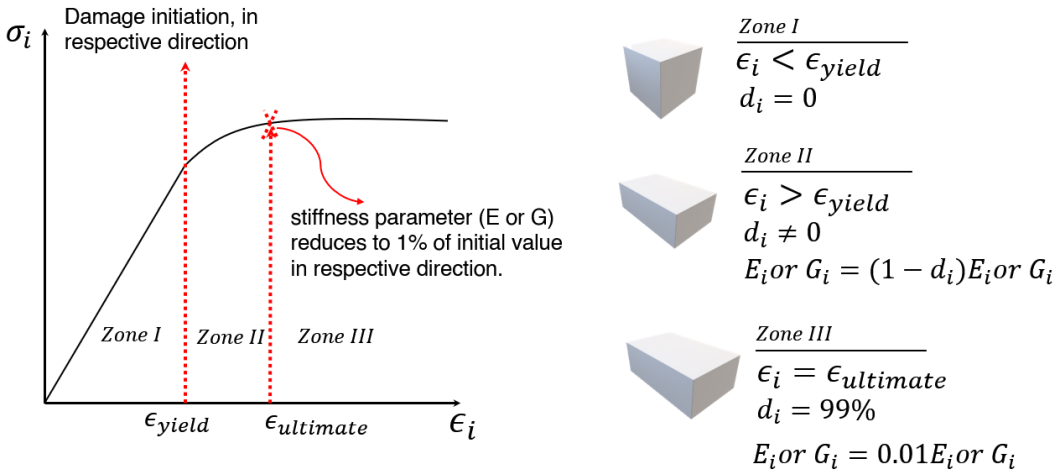

Figure 4.4. A typical stress-strain curve for an element with a damage model activated in the i-directions.

The linear damage model includes six damage parameters that independently affect the stiffness parameters in the respective direction. In each time step, the damage was computed automatically according to equation 10:

$$d_k = \max\left(d_k; D_k^c \left(\frac{\epsilon_k - \epsilon_k^s}{\epsilon_k^c - \epsilon_k^s}\right)_+\right) \qquad 10$$

In this equation, $()_+$ is the positive part of: $x_+ = \begin{cases} x & \text{if } x>0 \\ 0 & \text{if } x<0 \end{cases}$; ϵ_k^s and ϵ_k^c are yield and ultimate strains in the respective directions. The trabecular bone's stiffness and the ultimate strain were updated, and the material model remained isotropic elastic-plastic with a continuum damage mechanics parameter [110], [124].

4.3 Hyperelastic Material Models of Soft Tissue

The soft tissue is the main element for force attenuation during a fall incident. Consequently, it was essential to implement and validate a constitutive material model to represent each of the soft tissues in the hip segment. Three material models were implemented to investigate the model with the best correlation to the experiments. The first hyperelastic isotropic material model was the Ogden model [149], where the strain energy (W) was computed using equation 11:

$$W = \sum_{k=1}^{N} \frac{\mu_k}{\alpha_k} (\lambda_1^{\alpha_k} + \lambda_2^{\alpha_k} + \lambda_3^{\alpha_k} - 3) + \frac{1}{2} K (J-1)^2 \qquad 11$$

The Ogden parameters are represented with μ_k and α_k. K and J are bulk modulus and relative volume, and λ_i represents the principal stretches. The second model was Mooney-Rivlin [150], where the strain energy is calculated through equation 12:

$$W = \sum_{i+j>0}^{N} C_{ij}(I_1 - 3)^i (I_2 - 3)^j \quad 12$$

The C_{ij} are the material constants and I_1 and I_2 are the first and second invariants of the left Cauchy-Green tensor. The Prony series was used to implement the viscoelasticity effects into the models using equation 13:

$$G(t) = \sum_{i=1}^{N} G_i e^{\beta_i t} \quad 13$$

where G_i and β_i represent the shear relaxation moduli and the decay constants. Using equation 11 or 12, the stress tensor for the Ogden and Mooney-Rivlin models can be evaluated using the equations 14 and 15:

$$s_j = \lambda_j \frac{\partial W}{\partial \lambda_j} \quad 14$$

$$s = \frac{2}{J}\left[\frac{1}{J^{\frac{2}{3}}}\left(\frac{\partial W}{\partial I_1} + I_1 \frac{\partial W}{\partial I_2}\right)\boldsymbol{B} - \frac{1}{J^{\frac{4}{3}}}\frac{\partial W}{\partial I_2}\boldsymbol{B^2} - \frac{2}{3}\left(I_1 \frac{\partial W}{\partial I_1} + 2I_2 \frac{\partial W}{\partial I_2}\right)\boldsymbol{I}\right] \quad 15$$

where B is the left Cauchy-Green tensor, the s_j, s are the principal stress and stress, and I and J are unit of identity tensor and determinants of the deformation gradient. The last model was the quasilinear viscoelastic model (QLV) [77], [151], where the Cauchy stresses were calculated using the equation 16:

$$\sigma(t) = \sigma^e(0_+)G(t) + \int_0^t G(t-\tau) \times \frac{\partial \sigma^e[(\epsilon^*(\tau)]}{\partial \tau} d\tau \quad 16$$

where σ^e, G(t), and ϵ^* are the instantaneous elastic stress, reduced relaxation function, and the logarithmic strains, respectively.

4.4 Asphalt Material Modeling

The rubberized asphalt mixtures were developed at the University of Bologna, Italy. There were three different mixtures with 14, 28, and 33 weight percent rubber and a reference non-rubberized sample. Two mechanical tests were performed on the samples: non-destructive compression tests and destructive compression tests (Figure 4.5). The failure point in the destructive test was identified as a point where a visible deep crack was detected or when the force-deflection curve passed the global maximum force. The non-destructive compression test applied a 1% strain, and the destructive compression test continued until a visible crack appeared on the sample or the force-deflection curve passed the maximum force. Later, the mechanical compression tests were used to evaluate Young's modulus of the samples and implement the stress-strain curves into the *MAT_SIMPLIFIED_RUBBER material model in LS-Dyna [143]. The material model is a simple model that automatically computes the Ogden functional [149] using the provided stress-strain curves.

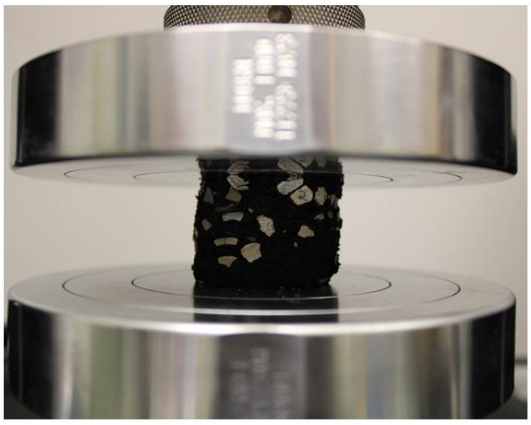

Figure 4.5. An asphalt mixture during the compression test.

The material model can govern the energy dissipation using two constants of hysteresis unloading (HU) and shape factor. These two constants were chosen to be 0.1 and 5, respectively (Figure 4.6). The material model for each asphalt mixture was validated using the standard HIC drop test results [152]. The drop tests were performed using a hemispheric impactor with weight and diameter of 4.6 kg and 160 mm, which were released from different heights.

(a)

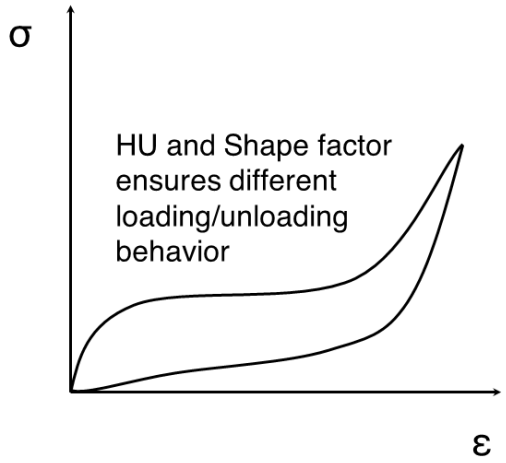

(b)

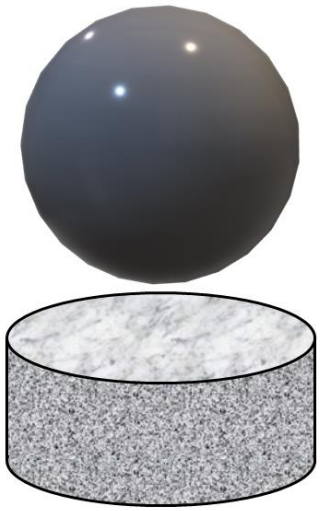

(c)

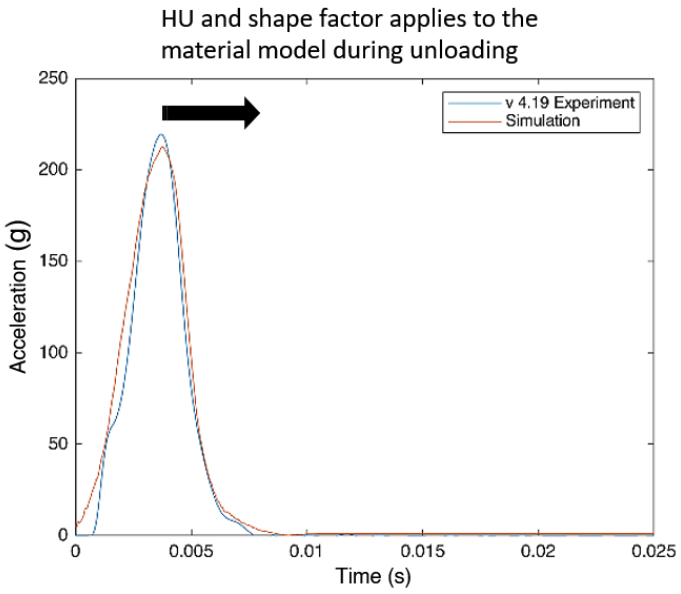

Figure 4.6. (a) A typical stress-strain curve for a *MAT_SIMPLIFIED_RUBBER model with non-zero HU/shape factors ensures a different unloading path [143], (b) a HIC drop test setup, (c) sample HIC drop test result on the asphalt mixture with 33% wt. rubber, the impact speed was 4.19 m/s. The unloading behavior of the material model is controlled by the HU and shape factor.

In addition to regular asphalt, the material model of the rubberized asphalt mixtures was compared to the playground material and a compliant playground material (Figure 4.7) [153], [154]. The compliant playground material was assumed to be five times softer than the regular playground material [153]. The material properties of the compliant playground are similar to Ethylene Propylene Diene Methyl (EPDM) foam (Figure 4.7) [155].

(a)

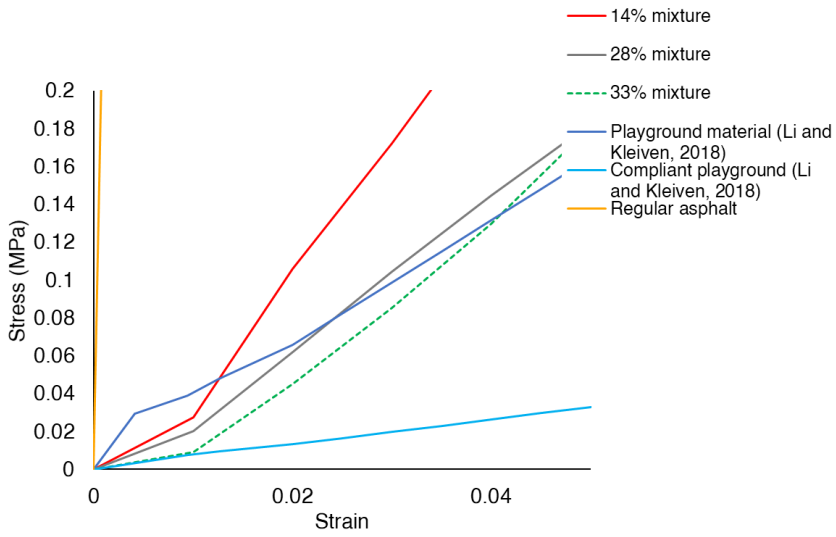

(b)

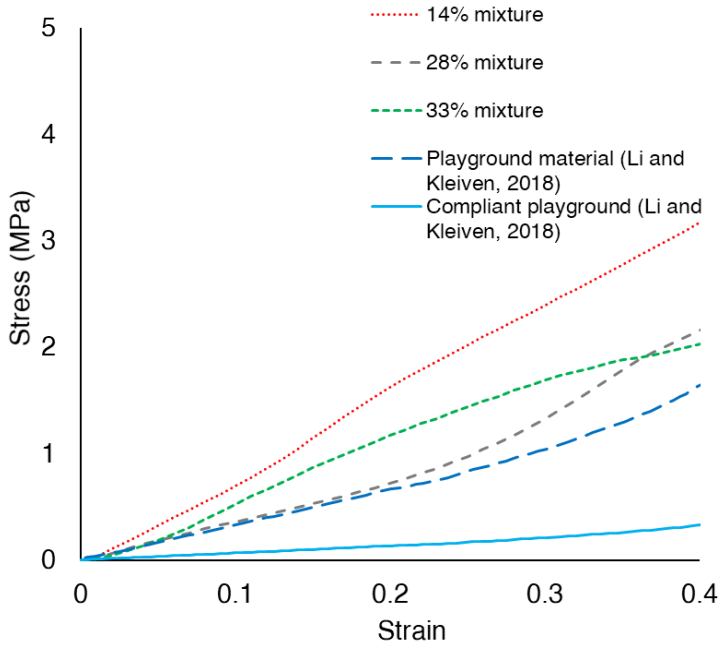

(c)

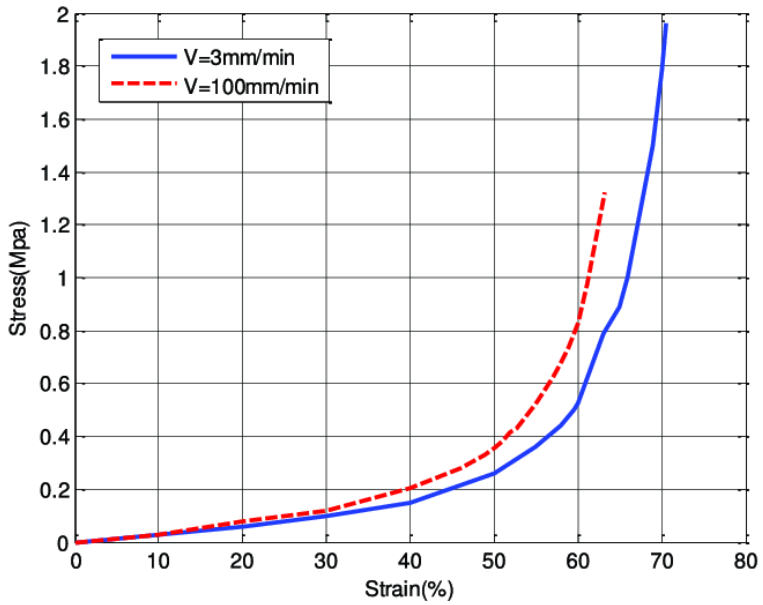

Figure 4.7. (a) Stress-strain curve (in elastic range) for different asphalt mixtures compared to the regular asphalt, playground material, and compliant playground material [156], (b) Stress-strain curve for different asphalt mixtures compared to the regular asphalt, playground material, and compliant playground material [156], (c) sample material (EPDM) with similar material properties as the compliant playground material [155] (The image is licensed under CC BY-NC-ND 3.0, which prohibits any remix, transform, or build upon).

5 Results

Each study's principal results are presented in the same order as the appended papers in the thesis. The first paper (paper A) addresses the effect of the different trunk and pelvis angles on the internal forces generated during a sideways fall. Section 5.2 presents the soft tissue material model results, which perform better in both external and internal forces according to the objective CORA rating (paper B). Next, the separate and combined effects of geometrical change and mechanical properties change due to aging in males and females are presented (paper C). In section5.4, the rubberized asphalt mixtures were implemented in two accident reconstruction simulations: a bicycle and a pedestrian accident case, to evaluate each mixture's ability in reducing the risk of head injuries (Paper D). Finally, the same asphalt mixtures were implemented in a fall incident identified in paper A to investigate the mixtures' ability to reduce the hip fracture risk (Paper E).

5.1 Paper A: Body Configuration

The whole-body model was positioned in the trunk angles ranging from 10 to 80 degrees and the pelvis angles ranging from -20 to +20 degrees. The trunk angle's highest internal forces occurred in the 10 degrees trunk angle for females and males (Figure 5.1). Similarly, the highest internal forces for the pelvis angle occurred in the +10 degrees pelvis rotation. The female model (weight 56 kg, height 156 cm) experienced relatively lower internal forces than the medium-size male model (weight 76 kg, height 177 cm) since it had a lower body weight.

(a)

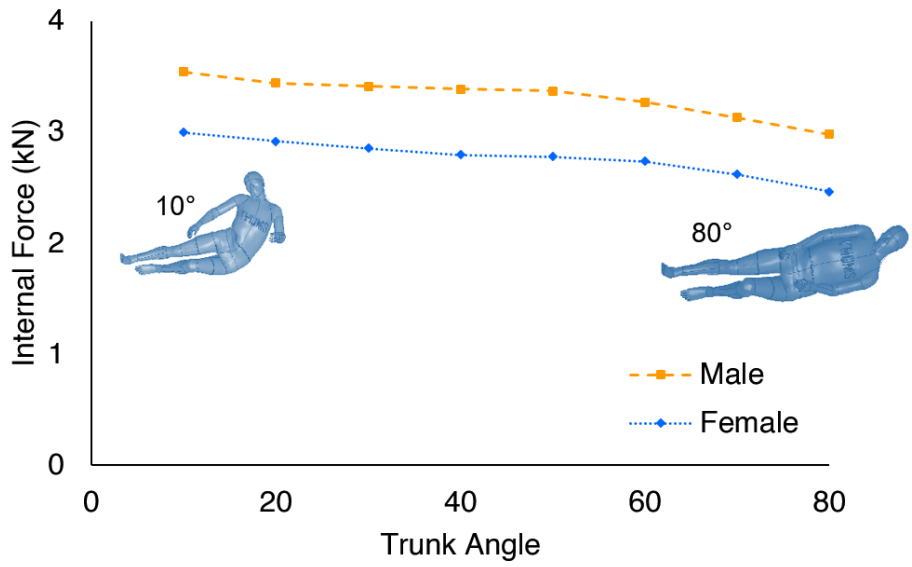

(b)

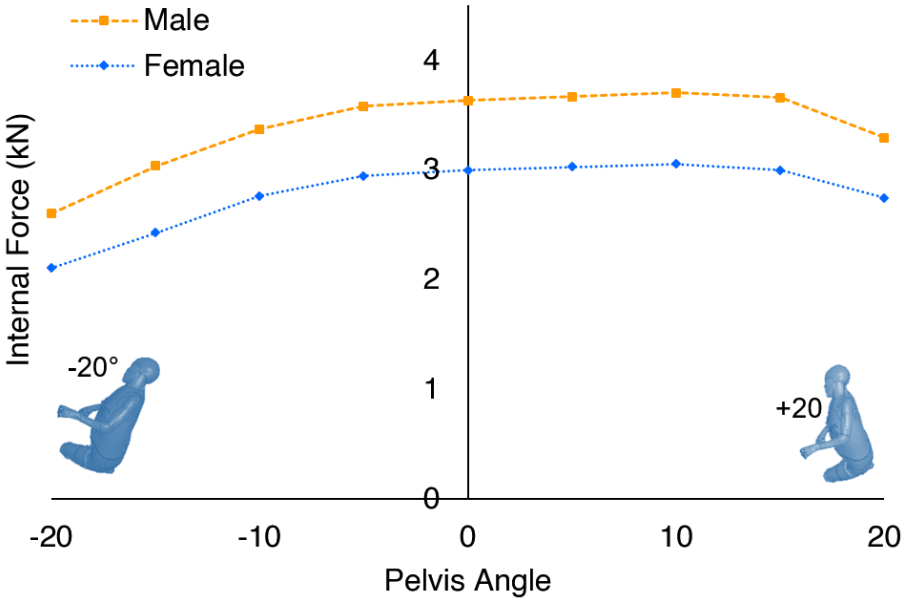

Figure 5.1. internal forces measured in the different trunk (a) and pelvis angles (b) for a male and a female finite element model [157].

5.2 Paper B: Objective Assessment of Soft Tissue Material Model

Adipose tissue material models were assessed objectively, using finite element simulation of a lateral hip impact. Three material models, from Brosch [71], Engelbrektsson [67], and Krouskop [68], had the highest CORA ratings (>0.8) for the 8 and 43mm soft tissue thicknesses. The Brosch model [71] had the closest maximum force prediction in both thicknesses, and all three models had lower energy dissipation than the experimental results for both thicknesses (Figure 5.2, a, b). Moreover, the internal forces increased 47 N for every 1 mm decrease in the soft tissue thickness when using the Brosch model [71].

(a)

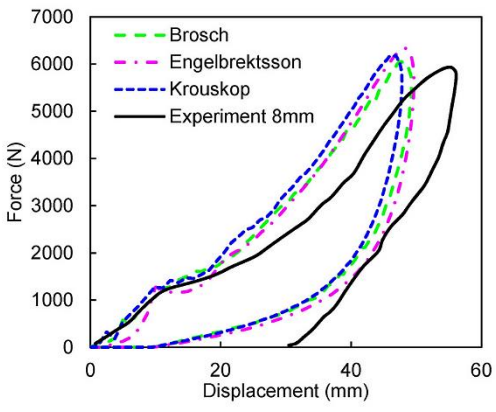

(b)

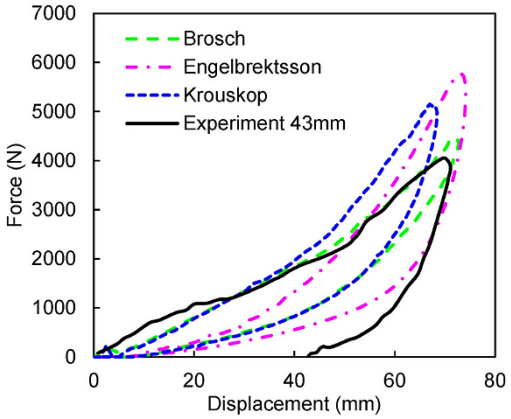

(c)

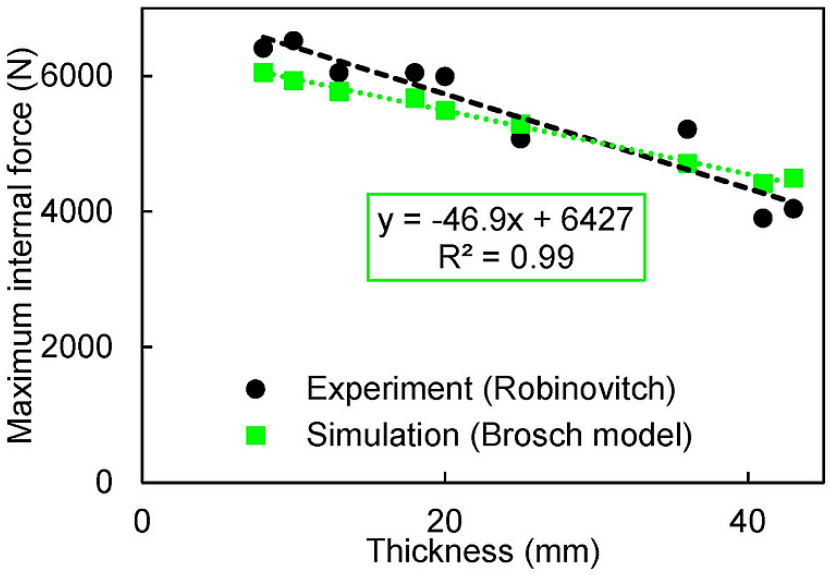

(d)

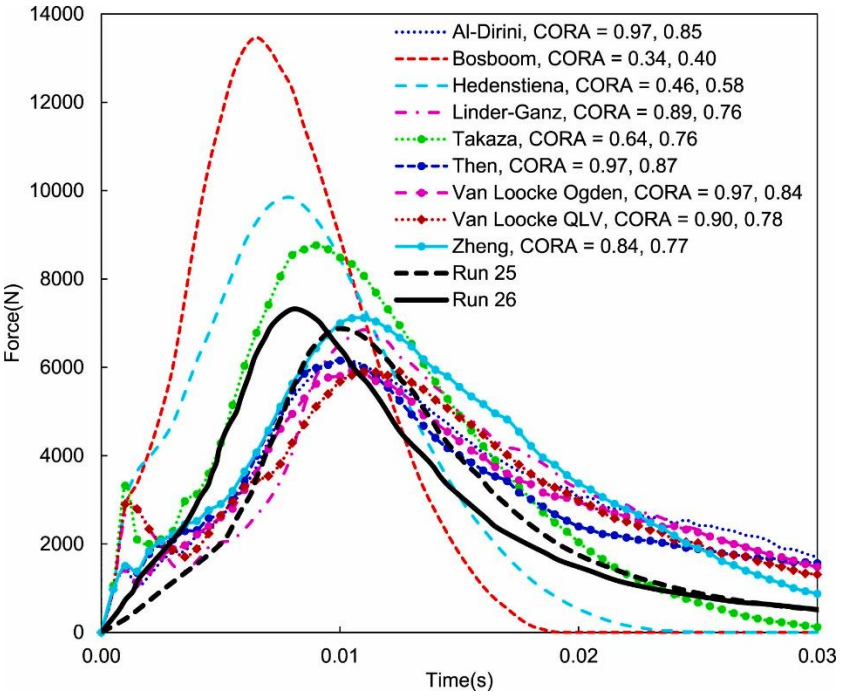

Figure 5.2. Force-displacement curves of the three adipose tissue material models for (a) 8 mm thickness, (b) 43 mm thickness, (c) maximum internal forces for different soft tissue thicknesses, (d) Force-time curves for different muscle material models, compared to the experimental results (Run 25 and Run 26) and their corresponding CORA ratings when compared with the each of the experiments (first reported number in the legend corresponds to Run 25) [54] (CC BY 4.0).

The adipose tissue material model with the highest rating was selected from the pelvis segment model to implement in the whole-body model to simulate lateral impacts to the hip (Figure 5.3). First, all muscle material models were compared to two experimental results (Figure 5.2, d), where three models with the highest CORA ratings were selected to simulate the rest of the experiments. The highest CORA rating among the three selected models occurred in the Ogden model based on

the experimental study by Van Loocke et al. [76], [77]. The CORA ratings for various constitutive models can be found in paper B in the appendix.

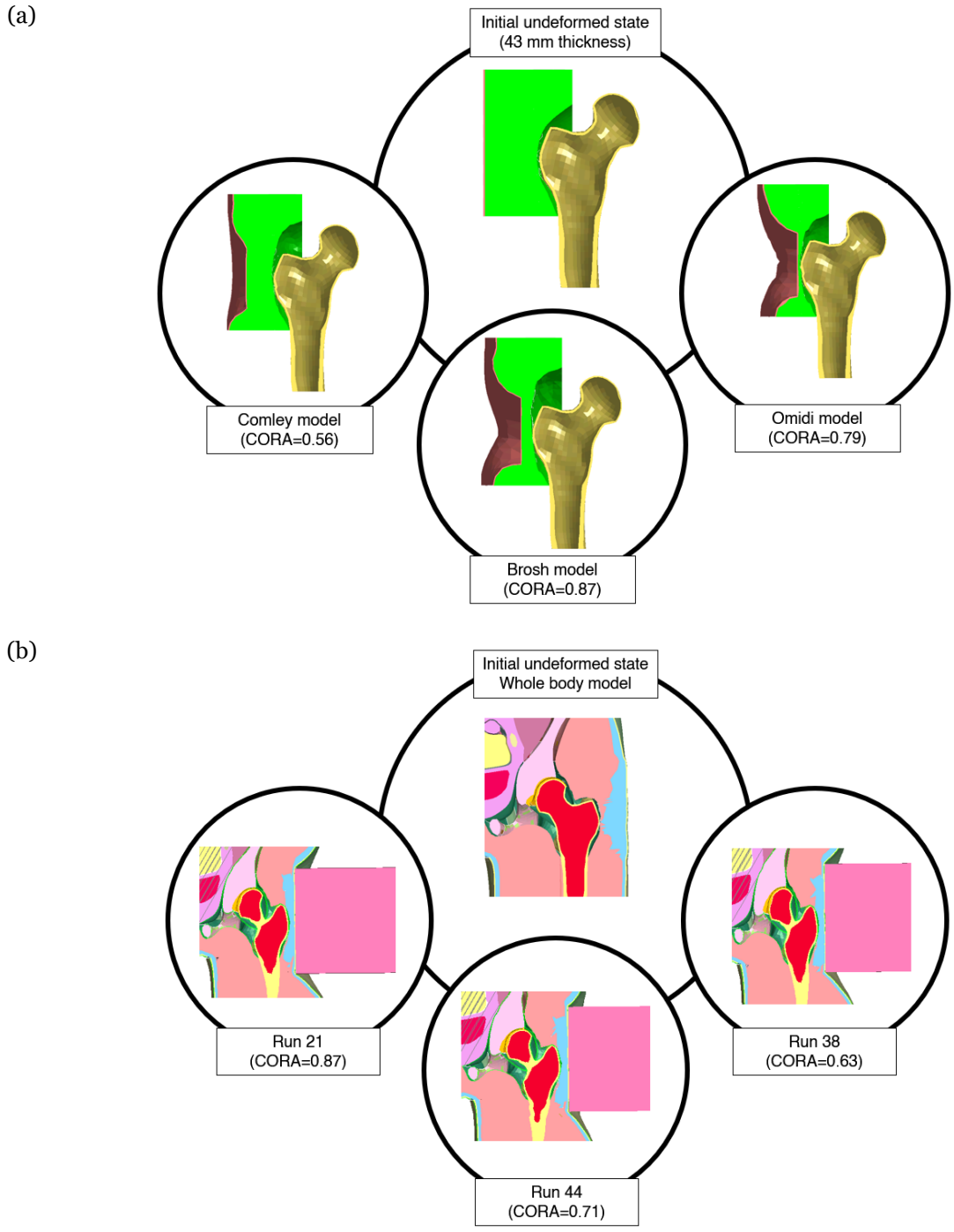

Figure 5.3. (a) Three sample CORA ratings for the adipose tissue material models and their corresponding deformation in the regional hip segment model, (b) the soft tissue deformations for the Van Loocke Ogden material model [76], [77] in three whole-body simulations with their corresponding deformations. The adipose tissue was modeled using the Brosh material model [71] (CC BY 4.0).

5.3 Paper C: Aging effects on the femoral strength

The changes in the proximal femur are age and sex dependent. The geometrical changes caused a 25 N/(decade of age) increase in the femoral strength for males, whereas it caused a 116 N/decade decrease for females. The mechanical properties change affected males and females differently even though the mechanical properties changes were implemented similarly. While the femoral strength decreased by about 354 N/decade for males, it only reduced by 225 N/decade for females. Finally, combining the geometrical changes and mechanical properties changes in both sexes caused 373 N/decade and 368 N/decade reductions in the femoral strength for the male and female models, respectively. It is noteworthy that the males experience a 7 percent decrease in femoral strength, whereas females experience an 11 percent reduction.

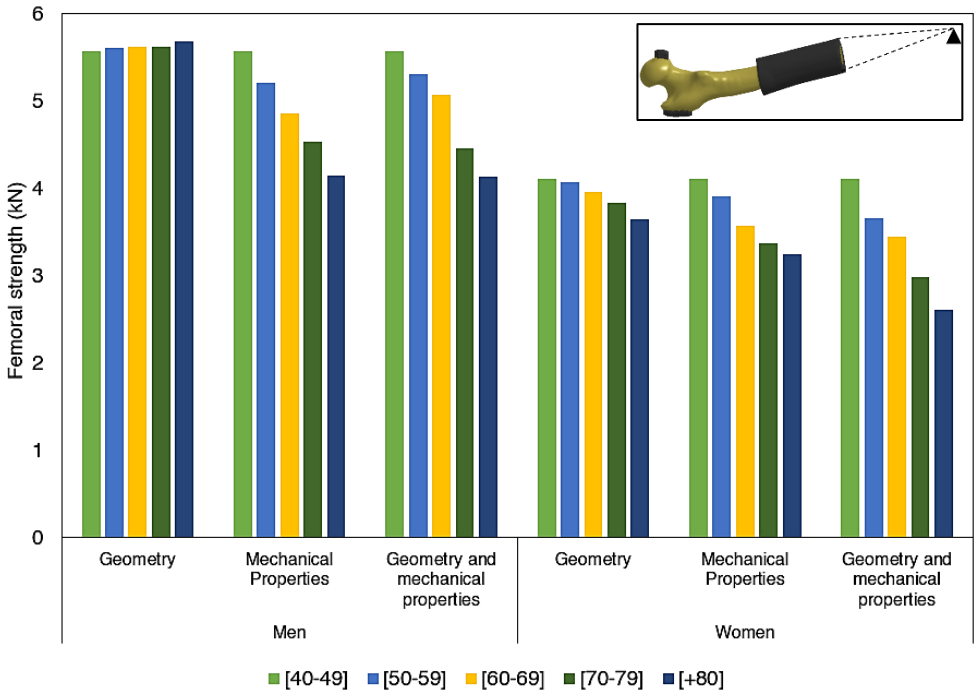

Figure 5.4. The femoral strength changes in the males and females due to separate and combined changes in the proximal femur's geometry and mechanical properties (CC BY 4.0).

5.4 Paper D: Risk of Head Injury on the Rubberized Asphalt

The three rubberized asphalt mixtures and two references, a non-rubberized asphalt and a playground material, were used to assess the rubberized asphalt mixtures' ability to reduce the head injury risk, i.e., skull fracture and concussion for two real case accidents. In the bicycle accident case, the sample with 33%wt rubber content had the lowest skull fracture risk among the rubberized asphalt mixtures (Figure 5.5). It is nevertheless the playground material that had the lowest risk of skull fracture. The sample with 33%wt rubber content had a concussion risk of 81 percent, similar to the playground material with 83%.

(a)

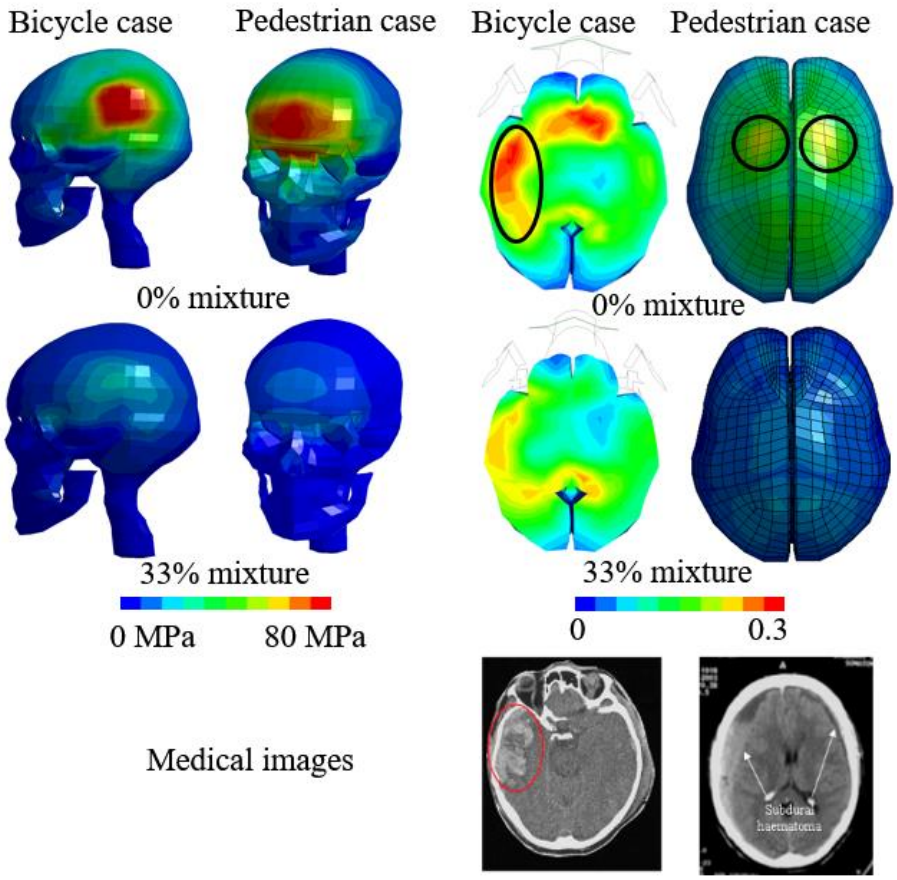

(b)

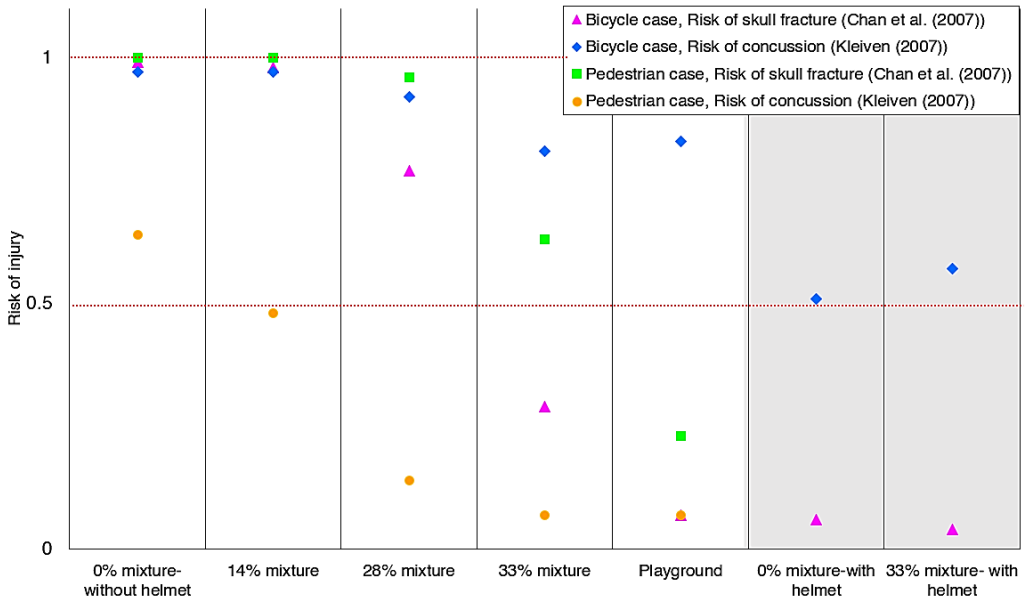

Figure 5.5. (a) Simulation results (left: stresses on the skull, right: strains in the brain tissue) for the bicycle and pedestrian accident cases; (b) risk of skull fracture and concussion for the bicycle and pedestrian accident cases; red dashed line indicates risks of 1.0 and 0.5 [158].

In the pedestrian case, the risk of skull fracture in the 33%wt asphalt mixture was 0.63 compared to the reference non-rubberized asphalt mixture (1.00). The 33%wt mixture's skull fracture performance was poorer than the playground material, reducing the risk to 0.23. However, the concussion risk was evaluated to be equal to 0.07 for the mixture with 33%wt rubber and the playground material (Figure 5.5).

5.5 Paper E: Risk of a Hip Fracture on the Rubberized Asphalt

The body posture which led to the highest internal forces in paper A was selected for simulation of the fall incident (Figure 5.6). In addition to the asphalt samples and the reference non-rubberized asphalt mixtures, playground material and a compliant playground material were also considered. The hip fracture risk was evaluated for the elderly male and female who fell on different asphalt mixtures. The internal forces were reduced by up to 10 percent for both male and female models in the rubberized asphalt mixtures. Based on the evaluated internal forces, the risk of hip fracture for an elderly male and an elderly female was computed. The potential risk of hip fracture for males was considerably low compared to females (about half). While the hip fracture risk was reduced to around 0.49 for the 33 %wt. rubber content mixture in the elderly female, it was reduced to 0.24 in the elderly male. The compliant playground material had the most risk reduction with the risk of 0.35 and 0.17 for the elderly females and males, respectively.

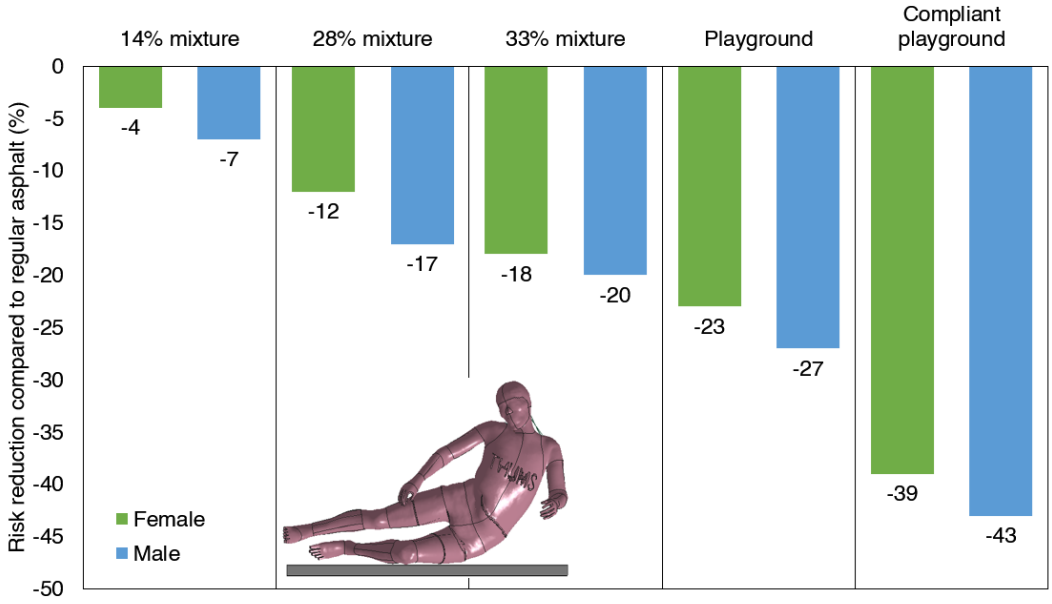

Figure 5.6. The reduction (%) of the hip fracture risk [100] for the elderly male and female when falling on the three asphalt mixtures and playground materials with respect to the reference non-rubberized asphalt mixture.

6 Discussion

Two main questions were asked at the beginning of the thesis. The first question was mainly aimed to investigate the parameters that can affect the fall outcome. The second question examined the hypothesis of the potential ability of the rubberized asphalt mixtures to reduce the risk of head or hip injuries. In this chapter, the two questions were discussed. Several limitations of the current work are also included in section 6.3.

6.1 How Are Different Parameters Affecting the Fall Outcome?

A brief answer to this question, according to the findings of studies A, B, and C, would be an 80-year-old female who falls on the rigid ground with an upright trunk angle (10°) and 10° anteriorly rotated pelvis, with a thin soft-tissue could experience a hip fracture when she falls. The four conditions that a fall can lead to a hip fracture were given in the background chapter [41] and quantitatively discussed in papers A, B, and C. A sideways fall that occurs to the hip segment (paper A); cannot be responded to with other body parts like the upper extremities in time (paper A); it cannot be attenuated with soft tissue covering the greater trochanter (paper B), and surpasses the proximal femur strength (paper C) leading to a hip fracture [41].

6.1.1 Body Posture

In paper A, different body postures regarding the trunk and pelvis angles were studied to identify the highest internal forces arising from a sideways fall. As the trunk angle changes from 10 degrees to 80 degrees, the internal force reduces. These changes in the internal forces can be explained by the effective mass and the soft tissue thickness. Dynamic and mathematical models suggest that the effective mass over the pelvis reduces as the body becomes more horizontal [44], [57], [159], [160]. Moreover, the trunk adduction stretches the soft tissues covering the femur's greater trochanteric area, which reduces the soft tissue thickness. A previous study suggested a 70 N increase of internal forces for each 1 mm decrease in the soft tissue thickness [56]. The internal force changes due to the pelvis rotation can be explained by other body parts' involvement and another thickness definition known as an effective soft tissue thickness. As the pelvis rotates towards the anterior, the lower extremities become more involved during the impact, and the initial impact occurs to the knee instead of the pelvis. This could absorb part of the impact energy. On the other hand, posterior rotation of the pelvis increases the involvement of the gluteus muscles and increases the chances of breaking the fall using the upper extremities. The gluteus muscles can increase the effective soft tissue thickness over the impact point and absorb more impact energy.

6.1.2 Soft Tissue

In paper B, different constitutive models for the muscle, adipose tissue, and skin were assessed to identify the model which can predict the internal and external forces during an impact on the hip

segment. The identification was made using an objective method named CORA rating. The soft tissue material model rated closer to 1 is a better predictor of the experimental results. The Ogden model for the muscle tissue was consistently rated higher than the other models [76], [78] for the external forces. The candidate adipose tissue and muscle material models [65]–[68], [71], [76], [77] were performing "good" to "excellent" in the internal and external forces according to ISO/TS 18571.

In addition to the constitutive models of adipose tissue and muscle, the soft tissue thickness covering the hip area can reduce the internal forces. Results [54] suggest that the internal forces reduce 47 N per 1 mm increase in the thickness, while the experimental result suggests a greater reduction of 70 N/mm [56].

6.1.3 Aging and Femoral Strength

In paper C, the aging effect on the strength of the proximal femur was investigated. The numerical method makes it possible to isolate the effects of the geometrical changes and mechanical properties changes for both males and females. The proximal femur strength reduces for females when accounting for the geometrical changes due to aging, whereas it slightly increases for males. This behavior is consistent with a longitudinal two-year cohort study's findings, which suggested a significant reduction of cortical cross-sectional area and moment of inertia in females [112]. The cortical cross-sectional area and moment of inertia changes were not directly changed in paper C; instead, the femoral neck width and the cortical thickness in each section around the femoral neck altered due to aging [107], [108], [114]. Increases in the neck width increase the moment of inertia and favorably the femoral strength, and regional thinning of the cortical thickness in superior sectors of the femoral neck reduces its strength [161], [162]. The apparent changes in mechanical properties due to aging are similar among males and females [163], [164], and it makes the cortical bone more brittle [120], [165], [166], which could explain the reduced femoral strength due to mechanical properties changes. Finally, the combined geometrical changes and mechanical properties changes due to aging causes a 10.7 percent decrease in females' femoral strength, whereas it decreases by 7.2 percent in males. The results of this paper were consistent with previous ageing studies on femoral strength [100], [111], [161], [167], [168].

6.2 Does Rubberized Asphalt Mixture Reduce the Injury Risk?

A very similar brief answer for this question will be if the 80-year-old female from the previous question (section 6.1) experiences a sideways fall on the 33%wt rubber content asphalt mixture, the hip fracture risk can be reduced by 20 percent (Paper E). Moreover, if the same female experiences a direct impact on the head, there would also be less brain concussion risk (paper D). Although the hip fracture risk in the softest asphalt mixture (33%wt) is 0.47 for the elderly female (the most vulnerable demographic), the other demographic groups, like elderly males, have less risk of hip fracture with the same asphalt mixture.

6.2.1 Head injury

Two cases were studied in paper D, a bicycle accident case and a pedestrian case. Increasing the rubber inside the mixtures improves the pavement's capability for reducing the risk of head injury. Wearing a helmet can reduce the brain strain by up to 48 percent during the bicycle accident case, while the asphalt mixture with 33%wt. rubber could reduce brain strains by up to 27 percent. The pedestrian case gained better results regarding brain strains and cortical bone stresses. The softest asphalt mixture (33% wt.) could reduce the brain strain up to 75 percent and the cortical bone stress

up to 50 percent. The brain concussion risk in the bicycle case was around 0.8 for the softest asphalt mixture and the playground material compared to regular asphalt, where the risk was about 1. Previous studies on the protective capacity of the playground materials [153], [169] showed a similar pattern concerning the risk of skull fracture and brain tissue injuries. The risk of skull fracture in the pedestrian case, which falls on the ground from approximately standing height, was about 0.64 for the softest asphalt mixture, and the risk of concussion was 0.07. The risk of concussion for the pedestrian case was about 0.64 for regular asphalt.

6.2.2 Hip fracture

In paper E, the hip fracture risk for an elderly female and male was evaluated. It was previously shown that females are at a higher risk of hip fracture [86], [99], [170]–[172]. Similarly, the risk of hip fracture for the elderly females in paper E was about twice that of elderly males when they fell on the rigid surface. The asphalt mixture with the highest rubber content reduced the hip fracture risk to 0.47 and 0.24 percent for elderly females and males. It was also shown that a compliant playground material could potentially reduce the risk of hip fracture for elderly females to 33 percent. There is still a debate on the effectiveness of interior flooring in preventing hip fractures in clinical studies. While some studies suggested a significant reduction in hip fractures in nursing homes with shock-absorbing flooring [135], [137], [138], a recent study found no such effect [139]. There is no previous study on the asphalt mixtures, and it seems to be challenging to make any inferences about the effectiveness of the rubberized asphalt pavements based on the clinical findings on floorings. It can be speculated that the rubberized asphalt mixture with the highest rubber content, which could reduce the risk of hip fracture to about 50 percent for the most vulnerable demographic group, can improve the pavements' preventive capacity for other demographic groups.

6.3 Limitations

There are several limitations in this thesis work. The parameters which could affect the fall outcome are not limited to the three parameters discussed in papers A, B, and C. In paper A, the body configurations were limited to trunk and pelvis angles as they were shown to be the major parameters [42], [43], [50]. In paper B, a unique soft tissue model did not outperform other models and the CORA ratings for several models, especially in the regional model, were "good." Moreover, the study did not consider the age effects or detailed muscle geometry or fiber directions [77], [125]. In paper C, the proximal femur model was taken from the THUMS model and was assumed to be homogenous, while CT-based models assume non-homogenous material properties and subject-specific geometry for assessment of the femoral strength [94], [173]–[175]. While those models are potentially more accurate for subject-specific strength assessment, there is no appropriate method to translate the subject-specific models to the population-based studies using the representative average whole-body models. Moreover, age was used as a representative parameter instead of BMD, porosity, mineral density, or T/Z-score to apply aging changes to the femur material model. Despite these limitations, the bone model was updated with a minimal change with respect to the THUMS model, making it possible to directly use the paper C to make the age-dependent THUMS model.

The second aspect of the thesis was to examine the protective effect of the rubberized asphalt mixtures. There are some limitations in this aspect of the thesis as well. A limited number of asphalt samples, both in number and variation of rubber contents (only 14, 28, and 33 %wt. rubber), were examined in this thesis. This limits practical conclusions for the recommended threshold of the rubber content to have optimized preventive effects. Moreover, the tests were done at a standard room temperature while the falls are more common during winter when the ground is colder [3]. The hip fracture risk for the asphalt mixture with the highest rubber content was similar to the playground material. This suggests that increasing the rubber content could have a limited effect on

reducing the risk of hip fracture further down. The studies in this phase of the thesis were limited to the asphalt mixtures' protective capability, whereas the balance, locomotion, mobility, and durability of the rubberized asphalt mixtures were not measured. Previous studies on shock-absorbing flooring suggest that locomotion and mobility could become an issue for the users [136] if the flooring is too soft.

Despite these limitations, the thesis presented comprehensive detail about fall biomechanics by studying the main parameters in sideways fall injuries. It examined the rubberized asphalt pavements' potential effect in reducing the risk of head injury or hip fracture. It is necessary to further study the rubberized asphalt pavements for their possible preventive capabilities and optimize them with respect to other characteristics of the pavements like durability.

7 Future Work

Several paths can be undertaken to improve the current thesis work. In the first aspect of the project, fall biomechanics, three major parameters were studied, and there are still some parameters that can affect the outcome of the fall, such as body mass index (BMI) or the activation of muscles [44], [55], [127]. In the second aspect, the rubberized asphalt mixtures, more parameters could be involved in the production, testing, and simulation processes, such as temperature and mobility.

The whole-body models are generalized average models and are suitable for population-based studies. Yet, they need to become more diverse to reflect wider intersubjective differences. In paper C, an aged proximal femur model was developed in order to reflect this need. The soft tissue thickness and material properties can be updated in future works. There are no specific experimental results for the material properties changes in the soft tissue due to aging other than a recent study measuring the soft tissue's stiffness in different age groups using an indentation device [125]. In this thesis, muscles were only modeled as passive tissues, whereas it is shown that the muscle activation in the hip region during a fall can affect the resultant forces [55]. The whole body model can be positioned in other relevant fall configurations, such as different knee positions for the impacting knee and the contralateral and upper extremity positions [176].

The rubberized asphalt mixtures were produced from crumb end-of-life tires. Although this method has environmental benefits by recycling the tires, it limits the injury prevention effects. It was shown in paper E that a compliant playground material could reduce the risk of hip fracture for small-size elderly females further than the highest rubber content of the asphalt mixture. In addition to more diverse asphalt mixtures, it is necessary to study the locomotion, mobility, and balance of these new asphalt mixtures. There is a need for a thorough optimization study to maximize the soft asphalt injury prevention capacity while the balance, locomotion, durability, and environmental friendliness of the asphalt mixture are kept within a reasonable threshold. Identification of the parameters needed for the optimization would be a challenge in itself. It would be better to study the temperature effect on injury prevention capacity of the asphalt mixtures in immediate future work. It is known that a fall is more common during winter when the mechanical properties of the asphalt mixtures could be affected by this parameter as well [3], [140].

8 Conclusion

The first three studies presented in the thesis were intended to improve the understanding of the sideways fall biomechanics by investigating the most relevant parameters to fall-induced hip fractures. The two later studies were intended to investigate the rubberized asphalt mixtures' effectiveness in preventing hip fracture by implementing the rubberized asphalt mixture material models into the THUMS finite element whole-body model. The separate conclusions of each study were presented below:

Paper A — In this paper, different body configurations were studied to investigate the trunk and pelvis angle, which leads to the highest internal forces evaluated on the femoral head for both males and females. The modified THUMS model from paper B was positioned at trunk angles ranging from 10 to 80 degrees. Later, the highest trunk angle was taken, and the pelvis rotated in the range of ±20 degrees (posteriorly and anteriorly). The internal forces were 17 percent higher for males compared to females in each of the trunk and pelvis angles. The 10 degrees trunk angle and 10 degrees anteriorly rotated pelvis lead to the femoral head's highest internal forces.

Paper B — In this paper, several nonlinear material models were selected to investigate the model which objectively has the highest CORA ratings for the adipose tissue in a regional model and the muscle in a whole-body model. First, the performance of the adipose tissue material models was compared in the regional model. The regional model only consists of a 100×100 adipose tissue sample with different thicknesses covering the greater trochanteric area. One adipose tissue was selected to be implemented in the whole-body model simulations. The Ogden model based on the previously published experimental study [76], [77] had higher ratings in the whole-body model simulations. Consequently, it could be a potential choice for the lateral impact simulations using the whole-body model.

Paper C — In this paper, the separate and combined effects of the geometrical and mechanical properties change on the femoral strength due to aging in males and females were investigated. Three sets of models were developed to address each of the changes separately and combined. The main geometrical changes were addressed with the expansion of the cortical width and inhomogeneous cortical thickness changes in both males and females. The mechanical properties changes were changed by reducing the Young's and shear modulus and reducing the ultimate strains. The combined geometrical changes and mechanical properties changes cause the femoral strength reduction for males and females; however, the geometrical changes reduced the femoral strength only for females. The geometrical changes slightly improve the strength in males. In all cases, females had lower femoral strength compared to males at the same age.

Paper D — In this paper, the effects of varying the rubber content on reducing the risk of skull fracture and brain concussion were assessed in two real case accident reconstructions. Three different asphalt mixtures with 14, 28, and 33 %wt rubber content were developed to identify the effect of increasing rubber content on reducing the risk of skull fracture and brain concussion. It was indicated that increasing the rubber content could improve asphalt mixtures' capacity in preventing skull fractures in the bicycle accident case. However, it only reduced the risk of brain concussion up to 16 percent in the same case. The asphalt mixture with the 33%wt rubber content had a better performance for the pedestrian accident case, where the brain concussion risk was around 7 percent (compared to 64 percent for the non-rubberized rigid asphalt). In this case, the same mixture's skull fracture risk is only reduced to 63 percent, which is still a high skull fracture risk compared to the playground material.

Paper E — In this paper, the effect of changing the rubber content was investigated in reducing the hip fracture risk in an elderly male and female. The whole-body model was positioned according to the results of paper A for both males and females. The same material models for the rubberized asphalt mixtures from paper D were implemented in the positioned whole-body male and female models. A playground material and a compliant playground material model were implemented along the rubberized asphalt mixtures to compare the risk of hip fractures better. The hip fracture risk was later evaluated using a hip fracture risk function for elderly males and females [100]. The risk of hip fracture for the asphalt sample with 33%wt rubber was about 0.5 for the elderly female and 0.24 percent for the elderly male. The compliant playground material had the best performance with reducing the risk of hip fracture down to 0.33 in the elderly female.

9 References

[1] World Health Organization (WHO), "WHO global report on falls prevention in older age," World Health Organization, Geneva, Switzerland, 2008.

[2] A. A. Zecevic, A. W. Salmoni, M. Speechley, and A. A. Vandervoort, "Defining a fall and reasons for falling: Comparisons among the views of seniors, health care providers, and the research literature," *Gerontologist*, vol. 46, no. 3. Gerontological Society of America, pp. 367–376, 2006.

[3] The Swedish Transport Administration, *Analysis of Road Safety Trends 2017*. The Swedish Transport Administration, 2018.

[4] A. F. Ambrose, G. Paul, and J. M. Hausdorff, "Risk factors for falls among older adults: A review of the literature," *Maturitas*, vol. 75, no. 1, pp. 51–61, May 2013.

[5] D. Houry, C. Florence, G. Baldwin, J. Stevens, and R. McClure, "The CDC Injury Center's Response to the Growing Public Health Problem of Falls Among Older Adults," *Am. J. Lifestyle Med.*, vol. 10, no. 1, pp. 74–77, Jan. 2016.

[6] L. Z. Rubenstein, "Falls in older people: Epidemiology, risk factors and strategies for prevention," in *Age and Ageing*, 2006, vol. 35, no. SUPPL.2.

[7] M. C. Nevitt and S. R. Cummings, "Type of Fall and Risk of Hip and Wrist Fractures: The Study of Osteoporotic Fractures," *J. Am. Geriatr. Soc.*, vol. 41, no. 11, pp. 1226–1234, Nov. 1993.

[8] J. P. Empana, P. Dargent-Molina, and G. Bréart, "Effect of Hip Fracture on Mortality in Elderly Women: The EPIDOS Prospective Study," *J. Am. Geriatr. Soc.*, vol. 52, no. 5, pp. 685–690, May 2004.

[9] Swedish Civil Contingencies Agency (MSB), "Social Costs of Accidents in Sweden," pp. 1–29, 2012.

[10] S. R. Cummings and L. J. Melton, "Osteoporosis I: Epidemiology and outcomes of osteoporotic fractures," *Lancet*, vol. 359, no. 9319. Elsevier Limited, pp. 1761–1767, 18-May-2002.

[11] J. A. Grisso, G. Y. Chiu, G. Maislin, W. C. Steinmann, and J. Portale, "Risk factors for hip fractures in men: A preliminary study," *J. Bone Miner. Res.*, vol. 6, no. 8, pp. 865–868, 1991.

[12] P. Kannus, J. Parkkari, H. Sievänen, A. Heinonen, I. Vuori, and M. Järvinen, "Epidemiology of hip fractures," in *Bone*, 1996, vol. 18, no. 1 SUPPL., pp. S57–S63.

[13] Centers for Disease Control and Prevention, "STEADI - Older Adult Fall Prevention | CDC

Injury Center," *centers for disease control and prevention*, 2018. [Online]. Available: https://www.cdc.gov/steadi/materials.html. [Accessed: 28-Mar-2018].

[14] A. Santacreu, "Safer City Streets Global Benchmarking for Urban Road Safety," Paris, Jan. 2018.

[15] World Health Organization (WHO), "Global Status Report on Road Safety 2018: Summary," Geneva, 2018.

[16] M. Rizzi, H. Stigson, and M. Krafft, "Cyclist Injuries Leading to Permanent Medical Impairment in Sweden and the Effect of Bicycle Helmets | Enhanced Reader," in *IRCOBI Conference*, 2013, pp. 412–423.

[17] M. Fahlstedt, P. Halldin, and S. Kleiven, "The protective effect of a helmet in three bicycle accidents - A finite element study," *Accid. Anal. Prev.*, vol. 91, pp. 135–143, Jun. 2016.

[18] C. S. Florence, G. Bergen, A. Atherly, E. Burns, J. Stevens, and C. Drake, "Medical Costs of Fatal and Nonfatal Falls in Older Adults," *J. Am. Geriatr. Soc.*, vol. 66, no. 4, pp. 693–698, Apr. 2018.

[19] E. R. Burns, J. A. Stevens, and R. Lee, "The direct costs of fatal and non-fatal falls among older adults — United States," *J. Safety Res.*, vol. 58, pp. 99–103, Sep. 2016.

[20] A. C. Laing and S. N. Robinovitch, "The force attenuation provided by hip protectors depends on impact velocity, pelvic size, and soft tissue stiffness," *J. Biomech. Eng.*, vol. 130, no. 6, p. 061005, Dec. 2008.

[21] A. C. Laing, F. Feldman, M. Jalili, C. M. (Jimmy) Tsai, and S. N. Robinovitch, "The effects of pad geometry and material properties on the biomechanical effectiveness of 26 commercially available hip protectors," *J. Biomech.*, vol. 44, no. 15, p. 2627, Oct. 2011.

[22] S. N. Robinovitch *et al.*, "Hip protectors: Recommendations for biomechanical testing-an international consensus statement (part I)," *Osteoporos. Int.*, vol. 20, no. 12, pp. 1977–1988, Dec. 2009.

[23] M. Fahlstedt *et al.*, "Influence of impact velocity and angle in a detailed reconstruction of a bicycle accident," in *IRCOBI Conference Proceedings - International Research Council on the Biomechanics of Injury*, 2012, pp. 787–799.

[24] M. Iwamoto and Y. Nakahira, "Development and Validation of the Total HUman Model for Safety (THUMS) Version 5 Containing Multiple 1D Muscles for Estimating Occupant Motions with Muscle Activation During Side Impacts," in *SAE Technical Papers*, 2015, no. November.

[25] M. Iwamoto, Y. Kisanuki, I. Watanabe, K. Furusu, and K. Miki, "Development of a finite element model of the total human model for safety (THUMS) and application to injury reconstruction," in *IRCOBI Conference Proceedings - International Research Council on the Biomechanics of Injury*, 2002, pp. 31–42.

[26] A. J. Golman, K. A. Danelson, L. E. Miller, and J. D. Stitzel, "Injury prediction in a side impact crash using human body model simulation," *Accid. Anal. Prev.*, 2014.

[27] S. L. Schoell *et al.*, "Development and Validation of an Older Occupant Finite Element Model of a Mid-Sized Male for Investigation of Age-related Injury Risk," in *Stapp car crash journal*, 2015, vol. 59, no. December, p. 359.

[28] M. L. Davis, B. Koya, J. M. Schap, and F. S. Gayzik, "Development and Full Body Validation of a 5th Percentile Female Finite Element Model," *SAE Tech. Pap.*, vol. 60, no. November,

pp. 509–544, 2016.

[29] S. Kleiven, “Evaluation of head injury criteria using a finite element model validated against experiments on localized brain motion, intracerebral acceleration, and intracranial pressure,” *Int. J. Crashworthiness*, vol. 11, no. 1, pp. 65–79, 2006.

[30] S. Kleiven, “Predictors for Traumatic Brain Injuries Evaluated through Accident Reconstructions,” in *SAE Technical Papers*, 2007, vol. 2007-Octob, no. October.

[31] Z. Zhou, X. Li, and S. Kleiven, “Fluid–structure interaction simulation of the brain–skull interface for acute subdural haematoma prediction,” *Biomech. Model. Mechanobiol.*, vol. 18, no. 1, pp. 155–173, Feb. 2019.

[32] C. Giordano and S. Kleiven, “Evaluation of Axonal Strain as a Predictor for Mild Traumatic Brain Injuries Using Finite Element Modeling,” in *SAE Technical Papers*, 2014, vol. 2014-November, no. November.

[33] Y. Dokko, O. Ito, and P. S. G. Co, “Development of Human Lower Limb and Pelvis FE Models for Adult and the Elderly,” in *SAE International*, 2009.

[34] J. P. Gaewsky *et al.*, “Modeling Human Volunteers in Multidirectional, Uni-axial Sled Tests Using a Finite Element Human Body Model,” *Ann. Biomed. Eng.*, vol. 47, no. 2, pp. 487–511, 2019.

[35] F. S. Gayzik, D. P. Moreno, N. A. Vavalle, A. C. Rhyne, and J. D. Stitzel, “Development of a Full Human Body Finite Element Model for Blunt Injury Prediction Utilizing a Multi-Modality Medical Imaging Protocol,” *12th Int’l LS-DYNA User Conf*, 2012.

[36] F. S. Gayzik, D. P. Moreno, C. P. Geer, S. D. Wuertzer, R. S. Martin, and J. D. Stitzel, “Development of a full body CAD dataset for computational modeling: A multi-modality approach,” *Ann. Biomed. Eng.*, vol. 39, no. 10, pp. 2568–2583, Oct. 2011.

[37] I. Fleps, A. Fung, P. Guy, S. J. Ferguson, B. Helgason, and P. A. Cripton, “Subject-specific ex vivo simulations for hip fracture risk assessment in sideways falls,” *Bone*, vol. 125, no. December 2018, pp. 36–45, 2019.

[38] I. Fleps, P. Guy, S. J. Ferguson, P. A. Cripton, and B. Helgason, “Explicit finite element models accurately predict subject-specific and velocity-dependent kinetics of sideways fall impact,” *J. Bone Miner. Res.*, 2019.

[39] W. S. Enns-Bray *et al.*, “Biofidelic finite element models for accurately classifying hip fracture in a retrospective clinical study of elderly women from the AGES Reykjavik cohort,” *Bone*, vol. 120, pp. 25–37, Mar. 2019.

[40] J. Parkkari *et al.*, “Majority of hip fractures occur as a result of a fall and impact on the greater trochanter of the femur: A prospective controlled hip fracture study with 206 consecutive patients,” *Calcif. Tissue Int.*, vol. 65, no. 3, pp. 183–187, 1999.

[41] S. R. Cummings and M. C. Nevitt, “A hypothesis: The causes of hip fractures,” *Journals Gerontol.*, vol. 44, no. 4, 1989.

[42] A. J. Van Den Kroonenberg, W. C. Hayes, and T. A. McMahon, “Hip impact velocities and body configurations for voluntary falls from standing height,” *J. Biomech.*, vol. 29, no. 6, pp. 807–811, Jun. 1996.

[43] F. Feldman and S. N. Robinovitch, “Reducing hip fracture risk during sideways falls: Evidence in young adults of the protective effects of impact to the hands and stepping,” *J. Biomech.*, vol. 40, no. 12, pp. 2612–2618, Jan. 2007.

[44] M. N. Sarvi, Y. Luo, P. Sun, and J. Ouyang, “Experimental Validation of Subject-Specific Dynamics Model for Predicting Impact Force in Sideways Fall,” *J. Biomed. Sci. Eng.*, vol. 7, no. 7, pp. 405–418, 2014.

[45] W. C. Hayes, E. R. Myers, S. N. Robinovitch, A. Van Den Kroonenberg, A. C. Courtney, and T. A. McMahon, “Etiology and prevention of age-related hip fractures,” *Bone*, vol. 18, no. 1, pp. S77–S86, Jan. 1996.

[46] M. Nasiri Sarvi and Y. Luo, “Sideways fall-induced impact force and its effect on hip fracture risk: a review,” *Osteoporos. Int.*, vol. 28, no. 10, pp. 2759–2780, Oct. 2017.

[47] E. S. Galliker, A. C. Laing, S. J. Ferguson, B. Helgason, and I. Fleps, “The Influence of Fall Direction and Hip Protector on Fracture Risk: FE Model Predictions Driven by Experimental Data,” *Ann. Biomed. Eng.*, vol. 50, no. 3, pp. 278–290, Mar. 2022.

[48] S. N. Robinovitch *et al.*, “Video capture of the circumstances of falls in elderly people residing in long-term care: an observational study,” *Lancet*, vol. 381, no. 9860, pp. 47–54, Jan. 2013.

[49] I. Fleps *et al.*, “A novel sideways fall simulator to study hip fractures ex vivo,” *PLoS One*, vol. 13, no. 7, p. e0201096, Jul. 2018.

[50] W. J. Choi and S. N. Robinovitch, “Effect of pelvis impact angle on stresses at the femoral neck during falls,” *J. Biomech.*, vol. 74, pp. 41–49, Jun. 2018.

[51] Henry Gray, *Anatomy of the Human Body*. Philadelphia: Lea & Febiger, 1918.

[52] J. G. Betts *et al.*, *Anatomy and phsiology*, vol. 53, no. 9. 2017.

[53] OpenStax College OpenStax CNX, “Anatomy and Physiology,” *OpenStax CNX*. [Online]. Available: http://cnx.org/contents/14fb4ad7-39a1-4eee-ab6e-3ef2482e3e22@11.1. [Accessed: 30-Jan-2021].

[54] P. Sahandifar and S. Kleiven, “Influence of nonlinear soft tissue modeling on the external and internal forces during lateral hip impacts,” *J. Mech. Behav. Biomed. Mater.*, vol. 124, p. 104743, Dec. 2021.

[55] W. J. Choi, P. A. Cripton, and S. N. Robinovitch, “Effects of hip abductor muscle forces and knee boundary conditions on femoral neck stresses during simulated falls,” *Osteoporos. Int.*, vol. 26, no. 1, pp. 291–301, Jan. 2015.

[56] S. N. Robinovitch, T. A. McMahon, and W. C. Hayes, “Force attenuation in trochanteric soft tissues during impact from a fall,” *J. Orthop. Res.*, vol. 13, no. 6, pp. 956–962, 1995.

[57] M. N. Sarvi, “Assessment of Hip Fracture Risk by a Two- Level Subject-Specific Biomechanical Model,” 2015.

[58] S. N. Robinovitch, W. C. Hayes, and T. A. McMahon, “Prediction of Femoral Impact Forces in Falls on the Hip,” *J. Biomech. Eng.*, vol. 113, no. 4, pp. 366–374, Nov. 1991.

[59] S. Majumder, A. Roychowdhury, and S. Pal, “Effects of trochanteric soft tissue thickness and hip impact velocity on hip fracture in sideways fall through 3D finite element simulations,” *J. Biomech.*, vol. 41, no. 13, pp. 2834–2842, Sep. 2008.

[60] S. Majumder, A. Roychowdhury, and S. Pal, “Hip fracture and anthropometric variations: Dominance among trochanteric soft tissue thickness, body height and body weight during sideways fall,” *Clin. Biomech.*, vol. 28, no. 9–10, pp. 1034–1040, Nov. 2013.

[61] I. C. Levine, L. E. Minty, and A. C. Laing, “Factors that influence soft tissue thickness over the greater trochanter: Application to understanding hip fractures,” *Clin. Anat.*, vol. 28, no. 2, pp. 253–261, Mar. 2015.

[62] M. L. Bouxsein, P. Szulc, F. Munoz, E. Thrall, E. Sornay-Rendu, and P. D. Delmas, “Contribution of trochanteric soft tissues to fall force estimates, the factor of risk, and prediction of hip fracture risk,” *J. Bone Miner. Res.*, vol. 22, no. 6, pp. 825–831, Mar. 2007.

[63] F. L.-S. Goh, “Wearable Hip Protectors : Validation of a Novel Test System and Evaluation Utilizing Pressure Sensing Methods by,” 2017.

[64] H. Seok, Y. T. Kim, S. H. Kim, and J. G. Cha, “Treatment of Transient Osteoporosis of the Hip with Intravenous Zoledronate - A Case Report -,” *Ann. Rehabil. Med.*, vol. 35, no. 3, p. 432, 2011.

[65] R. M. A. Al-Dirini, M. P. Reed, J. Hu, and D. Thewlis, “Development and Validation of a High Anatomical Fidelity FE Model for the Buttock and Thigh of a Seated Individual,” *Ann. Biomed. Eng.*, vol. 44, no. 9, pp. 2805–2816, Sep. 2016.

[66] C. Then *et al.*, “A method for a mechanical characterisation of human gluteal tissue,” *Technol. Heal. Care*, vol. 15, no. 6, pp. 385–398, 2007.

[67] K. Engelbrektsson, “Evaluation of material models in LS-DYNA for impact simulation of white adipose tissue,” 2011.

[68] T. A. Krouskop, T. M. Wheeler, F. Kallel, B. S. Garra, and T. Hall, “Elastic moduli of breast and prostate tissues under compression,” *Ultrason. Imaging*, vol. 20, no. 4, pp. 260–274, Oct. 1998.

[69] E. Omidi, L. Fuetterer, S. Reza Mousavi, R. C. Armstrong, L. E. Flynn, and A. Samani, “Characterization and assessment of hyperelastic and elastic properties of decellularized human adipose tissues,” *J. Biomech.*, vol. 47, no. 15, pp. 3657–3663, Nov. 2014.

[70] K. Comley and N. Fleck, “The compressive response of porcine adipose tissue from low to high strain rate,” *Int. J. Impact Eng.*, vol. 46, pp. 1–10, 2012.

[71] T. Brosh and M. Arcan, “Modeling the body/chair interaction - An integrative experimental-numerical approach,” *Clin. Biomech.*, vol. 15, no. 3, pp. 217–219, Mar. 2000.

[72] S. Hedenstierna, P. Halldin, and K. Brolin, “Evaluation of a combination of continuum and truss finite elements in a model of passive and active muscle tissue,” *Comput. Methods Biomech. Biomed. Engin.*, vol. 11, no. 6, pp. 627–639, 2014.

[73] E. Linder-Ganz, N. Shabshin, Y. Itzchak, and A. Gefen, “Assessment of mechanical conditions in sub-dermal tissues during sitting: A combined experimental-MRI and finite element approach,” *J. Biomech.*, vol. 40, no. 7, pp. 1443–1454, 2007.

[74] R. Pietsch *et al.*, “Anisotropic compressive properties of passive porcine muscle tissue,” *J. Biomech. Eng.*, vol. 136, no. 11, pp. 1–7, 2014.

[75] M. Takaza, K. M. Moerman, and C. K. Simms, “Passive skeletal muscle response to impact loading: Experimental testing and inverse modelling,” *J. Mech. Behav. Biomed. Mater.*, vol. 27, pp. 214–225, 2013.

[76] M. Van Loocke, C. G. Lyons, and C. K. Simms, “A validated model of passive muscle in compression,” *J. Biomech.*, vol. 39, no. 16, pp. 2999–3009, 2006.

[77] M. Van Loocke, C. G. Lyons, and C. K. Simms, “Viscoelastic properties of passive skeletal

muscle in compression: Stress-relaxation behaviour and constitutive modelling," *J. Biomech.*, vol. 41, no. 7, pp. 1555–1566, 2008.

[78] Y. Zheng, A. F. T. Mak, and B. Lue, "Objective assessment of limb tissue elasticity: Development of a manual indentation procedure," *J. Rehabil. Res. Dev.*, vol. 36, no. 2, pp. 71–85, 1999.

[79] F. M. Hendriks, D. Brokken, J. T. W. M. van Eemeren, C. W. J. Oomens, F. P. T. Baaijens, and J. B. A. M. Horsten, "A numerical-experimental method to characterize the non-linear mechanical behavior of human skin," *Ski. Res. Technol.*, vol. 9, no. 3, pp. 274–283, 2003.

[80] S. S. Chen, Y. H. Falcovitz, R. Schneiderman, A. Maroudas, and R. L. Sah, "Depth-dependent compressive properties of normal aged human femoral head articular cartilage: Relationship to fixed charge density," *Osteoarthr. Cartil.*, vol. 9, no. 6, pp. 561–569, 2001.

[81] Z. Li, J. E. Kim, J. S. Davidson, B. S. Etheridge, J. E. Alonso, and A. W. Eberhardt, "Biomechanical response of the pubic symphysis in lateral pelvic impacts: A finite element study," *J. Biomech.*, vol. 40, no. 12, pp. 2758–2766, 2007.

[82] G. J. Dakin, R. A. Arbelaez, F. J. Molz IV, J. E. Alonso, K. A. Mann, and A. W. Eberhardt, "Elastic and viscoelastic properties of the human pubic symphysis joint: Effects of lateral impact loading," *J. Biomech. Eng.*, vol. 123, no. 3, pp. 218–226, Jun. 2001.

[83] J. D. Hewitt, R. R. Glisson, F. Guilak, and T. P. Vail, "The mechanical properties of the human hip capsule ligaments," *J. Arthroplasty*, vol. 17, no. 1, pp. 82–89, 2002.

[84] J. Hewitt, F. Guilak, R. Glisson, and T. P. Vail, "Regional material properties of the human hip joint capsule ligaments," *J. Orthop. Res.*, vol. 19, no. 3, pp. 359–364, 2001.

[85] I. Fleps, W. S. Enns-Bray, P. Guy, S. J. Ferguson, P. A. Cripton, and B. Helgason, "On the internal reaction forces, energy absorption, and fracture in the hip during simulated sideways fall impact," *PLoS One*, vol. 13, no. 8, p. e0200952, Aug. 2018.

[86] F. Johannesdottir, E. Thrall, J. Muller, T. M. Keaveny, D. L. Kopperdahl, and M. L. Bouxsein, "Comparison of non-invasive assessments of strength of the proximal femur," *Bone*, vol. 105, pp. 93–102, Dec. 2017.

[87] S. Nawathe, B. P. Nguyen, N. Barzanian, H. Akhlaghpour, M. L. Bouxsein, and T. M. Keaveny, "Cortical and trabecular load sharing in the human femoral neck," *J. Biomech.*, vol. 48, no. 5, pp. 816–822, 2015.

[88] S. L. Manske *et al.*, "Cortical and trabecular bone in the femoral neck both contribute to proximal femur failure load prediction," *Osteoporos Int*, vol. 20, pp. 445–453, 2009.

[89] G. Holzer *et al.*, "Hip Fractures and the Contribution of Cortical Versus Trabecular Bone to Femoral Neck Strength," *J. Bone Miner. Res.*, vol. 2424, no. 3, pp. 468–474, Mar. 2009.

[90] R. B. B. Ashman, S. C. C. Cowin, W. C. C. Van Buskirk, J. C. Rice, and J. C. Rice+, "A continuous wave technique for the measurement of the elastic properties of cortical bone," *J. Biomech.*, vol. 17, no. 5, pp. 349–361, Jan. 1984.

[91] D. T. Reilly, A. H. Burstein, and V. H. Frankel, "The elastic modulus for bone," *J. Biomech.*, vol. 7, no. 3, pp. 271–275, May 1974.

[92] D. T. Reilly and A. H. Burstein, "The elastic and ultimate properties of compact bone tissue," *J. Biomech.*, vol. 8, no. 6, pp. 393–405, Jan. 1975.

[93] J. Currey, "Incompatible mechanical properties in compact bone," *J. Theor. Biol.*, vol. 231,

no. 4, pp. 569–580, Dec. 2004.

[94] H. H. Bayraktar, E. F. Morgan, G. L. Niebur, G. E. Morris, E. K. Wong, and T. M. Keaveny, “Comparison of the elastic and yield properties of human femoral trabecular and cortical bone tissue,” *J. Biomech.*, vol. 37, no. 1, pp. 27–35, 2004.

[95] C. H. Turner, J. Rho, Y. Takano, T. Y. Tsui, and G. M. Pharr, “The elastic properties of trabecular and cortical bone tissues are similar: results from two microscopic measurement techniques,” *J. Biomech.*, vol. 32, pp. 437–441, 1999.

[96] W. S. Enns-Bray, J. S. Owoc, K. K. Nishiyama, and S. K. Boyd, “Mapping anisotropy of the proximal femur for enhanced image based finite element analysis,” *J. Biomech.*, vol. 47, no. 13, pp. 3272–3278, Oct. 2014.

[97] P. Sahandifar and S. Kleiven, “Separate and Combined Effects of Geometrical and Mechanical Properties Changes Due to Aging on the Femoral Strength in Men and Women,” *Front. Mech. Eng.*, vol. 7, p. 1, May 2021.

[98] A. C. Courtney, E. F. Wachtel, E. R. Myers, and W. C. Hayes, “Effects of Loading Rate on Strength of the Proximal Femur,” *Calcif Tissue Int*, vol. 55, no. 1, pp. 53–58, 1994.

[99] D. Dragomir-Daescu *et al.*, “Robust QCT/FEA Models of Proximal Femur Stiffness and Fracture Load During a Sideways Fall on the Hip,” *Ann. Biomed. Eng.*, vol. 39, no. 2, pp. 742–755, Feb. 2011.

[100] S. Kleiven, “Hip fracture risk functions for elderly men and women in sideways falls,” *J. Biomech.*, vol. 105, p. 109771, May 2020.

[101] M. J. Silva, “Biomechanics of osteoporotic fractures,” *Injury*, vol. 38, no. 3, pp. 69–76, Sep. 2007.

[102] E. F. Morgan and M. L. Bouxsein, “Biomechanics of Bone and Age-Related Fractures,” in *Principles of Bone Biology*, J. P. Bilezikian, L. G. Raisz, and T. J. Martin, Eds. Academic Press, 2008, pp. 29–51.

[103] L. Grassi *et al.*, “Accuracy of finite element predictions in sideways load configurations for the proximal human femur,” *J. Biomech.*, vol. 45, no. 2, pp. 394–399, Jan. 2012.

[104] J. Panyasantisuk, E. Dall’Ara, M. Pretterklieber, D. H. Pahr, and P. K. Zysset, “Mapping anisotropy improves QCT-based finite element estimation of hip strength in pooled stance and side-fall load configurations,” *Med. Eng. Phys.*, vol. 59, pp. 36–42, Sep. 2018.

[105] A. C. Courtney, E. F. Wachtel, E. R. Myers, and W. C. Hayes, “Age-related reductions in the strength of the femur tested in a fall- loading configuration,” *J. Bone Jt. Surg. - Ser. A*, vol. 77, no. 3, pp. 387–395, 1995.

[106] A. Rezaei and D. Dragomir-Daescu, “Femoral Strength Changes Faster with Age Than BMD in Both Women and Men: A Biomechanical Study,” *J. Bone Miner. Res.*, vol. 30, no. 12, pp. 2200–2206, 2015.

[107] F. Johannesdottir *et al.*, “Similarities and differences between sexes in regional loss of cortical and trabecular bone in the mid-femoral neck: The AGES-Reykjavik longitudinal study,” *J. Bone Miner. Res.*, vol. 28, no. 10, pp. 2165–2176, Oct. 2013.

[108] P. M. Mayhew *et al.*, “Relation between age, femoral neck cortical stability, and hip fracture risk,” *Lancet*, vol. 366, no. 9480, pp. 129–135, Jul. 2005.

[109] I. Ott, R. Kienzler, and R. Schröder, “Aging in the cortical bone: a constitutive law and its

application," *Arch. Appl. Mech.*, vol. 80, no. 5, pp. 527–541, May 2010.

[110] T. M. Keaveny, "Cancellous bone," in *Handbook of Biomaterial Properties*, Boston, MA: Springer US, 1998, pp. 15–23.

[111] D. Dragomir-Daescu *et al.*, "Factors associated with proximal femur fracture determined in a large cadaveric cohort," *Bone*, vol. 116, no. August, pp. 196–202, 2018.

[112] M. Ito, T. Nakata, A. Nishida, and M. Uetani, "Age-related changes in bone density, geometry and biomechanical properties of the proximal femur: CT-based 3D hip structure analysis in normal postmenopausal women," *Bone*, vol. 48, no. 3, pp. 627–630, Mar. 2011.

[113] R. D. Carpenter *et al.*, "Effects of age and sex on the strength and cortical thickness of the femoral neck," *Bone*, vol. 48, no. 4, pp. 741–747, Apr. 2011.

[114] T. J. Beck *et al.*, "Structural Trends in the Aging Femoral Neck and Proximal Shaft: Analysis of the Third National Health and Nutrition Examination Survey Dual-Energy X-Ray Absorptiometry Data," *J. Bone Miner. Res.*, vol. 15, no. 12, pp. 2297–2304, Dec. 2000.

[115] F. Johannesdottir *et al.*, "Distribution of cortical bone in the femoral neck and hip fracture: A prospective case-control analysis of 143 incident hip fractures; the AGES-REYKJAVIK Study," *Bone*, vol. 48, no. 6, pp. 1268–1276, Jun. 2011.

[116] K. E. S. Poole *et al.*, "Cortical Thickness Mapping to Identify Focal Osteoporosis in Patients with Hip Fracture," *PLoS One*, vol. 7, no. 6, p. e38466, Jun. 2012.

[117] K. E. Poole *et al.*, "Changing structure of the femoral neck across the adult female lifespan," *J. Bone Miner. Res.*, vol. 25, no. 3, pp. 482–491, Mar. 2010.

[118] J. Carballido-Gamio *et al.*, "Structural patterns of the proximal femur in relation to age and hip fracture risk in women," *Bone*, vol. 57, no. 1, pp. 290–299, Nov. 2013.

[119] B. C. C. Khoo, K. Brown, J. R. Lewis, E. Perilli, and R. L. Prince, "Ageing Effects on 3-Dimensional Femoral Neck Cross-Sectional Asymmetry: Implications for Age-Related Bone Fragility in Falling," *J. Clin. Densitom.*, vol. 22, no. 2, pp. 153–161, 2019.

[120] B. Martin, "Aging and strength of bone as a structural material," *Calcif. Tissue Int.*, vol. 53, no. Suppl 1, pp. S34–S40, Feb. 1993.

[121] G. Osterhoff, E. F. Morgan, S. J. Shefelbine, L. Karim, L. M. McNamara, and P. Augat, "Bone mechanical properties and changes with osteoporosis," *Injury*, vol. 47, no. Suppl 2, pp. S11–S20, 2016.

[122] M. Kutz, *Biomedical Engineering and design handbook, Volume 1*, vol. 1. New York: McGraw-Hill, 2009.

[123] M. J. Mirzaali *et al.*, "Mechanical properties of cortical bone and their relationships with age, gender, composition and microindentation properties in the elderly," *Bone*, vol. 93, pp. 196–211, 2016.

[124] L. L. Mosekilde, L. L. Mosekilde, and C. C. Danielsen, "Biomechanical competence of vertebral trabecular bone in relation to ash density and age in normal individuals," *Bone*, vol. 8, no. 2, pp. 79–85, 1987.

[125] W. J. Choi, C. M. Russell, C. M. Tsai, S. Arzanpour, and S. N. Robinovitch, "Age-related changes in dynamic compressive properties of trochanteric soft tissues over the hip," *J. Biomech.*, vol. 48, no. 4, pp. 695–700, Feb. 2015.

[126] W. J. Choi, J. M. Wakeling, and S. N. Robinovitch, “Kinematic analysis of video-captured falls experienced by older adults in long-term care,” *J. Biomech.*, vol. 48, no. 6, pp. 911–920, Apr. 2015.

[127] W. J. Choi, J. A. Hoffer, and S. N. Robinovitch, “Effect of hip protectors, falling angle and body mass index on pressure distribution over the hip during simulated falls,” *Clin. Biomech.*, vol. 25, no. 1, pp. 63–69, Jan. 2010.

[128] B. E. Groen, V. Weerdesteyn, and J. Duysens, “Martial arts fall techniques decrease the impact forces at the hip during sideways falling,” *J. Biomech.*, vol. 40, no. 2, pp. 458–462, 2007.

[129] V. Wallqvist and L. Kraft, “Prototype bike lanes - placement practices and properties,” in *3rd international conference on best practices for concrete pavements*, 2015, no. October 2015.

[130] P. Kannus, J. Parkkari, and J. Poutala, “Comparison of force attenuation properties of four different hip protectors under simulated falling conditions in the elderly: An in vitro biomechanical study,” *Bone*, vol. 25, no. 2, pp. 229–235, Aug. 1999.

[131] N. M. van Schoor, A. J. van der Veen, L. A. Schaap, T. H. Smit, and P. Lips, “Biomechanical comparison of hard and soft hip protectors, and the influence of soft tissue,” *Bone*, vol. 39, no. 2, pp. 401–407, Aug. 2006.

[132] S. N. Robinovitch, W. C. Hayes, and T. A. Mcmahon, “Distribution of Contact Force during Impact to the Hip,” *Ann. Biomed. Eng.*, vol. 25, no. 3, pp. 499–508, 1997.

[133] W. J. Choi, J. A. Hoffer, and S. N. Robinovitch, “The effect of positioning on the biomechanical performance of soft shell hip protectors,” *J. Biomech.*, vol. 43, no. 5, pp. 818–825, Mar. 2010.

[134] B. E. Keenan and S. L. Evans, “Biomechanical testing of hip protectors following the Canadian Standards Association express document,” *Osteoporos. Int.*, vol. 30, no. 6, pp. 1205–1214, Apr. 2019.

[135] J. Gustavsson, C. Bonander, R. Andersson, and F. Nilson, “Investigating the fall-injury reducing effect of impact absorbing flooring among female nursing home residents: Initial results,” *Inj. Prev.*, vol. 21, no. 5, pp. 320–324, Oct. 2015.

[136] A. C. Laing and S. N. Robinovitch, “Low stiffness floors can attenuate fall-related femoral impact forces by up to 50% without substantially impairing balance in older women,” *Accid. Anal. Prev.*, vol. 41, no. 3, pp. 642–650, May 2009.

[137] A. K. Drahota *et al.*, “Pilot cluster randomised controlled trial of flooring to reduce injuries from falls in wards for older people,” *Age Ageing*, vol. 42, no. 5, pp. 633–640, 2013.

[138] F. Knoefel, L. Patrick, J. Taylor, and R. Goubran, “Dual-Stiffness Flooring: Can It Reduce Fracture Rates Associated With Falls?,” *J. Am. Med. Dir. Assoc.*, vol. 14, no. 4, pp. 303–305, Apr. 2013.

[139] D. C. Mackey *et al.*, “The Flooring for Injury Prevention (FLIP) Study of compliant flooring for the prevention of fall-related injuries in long-term care: A randomized trial,” *PLOS Med.*, vol. 16, no. 6, p. e1002843, Jun. 2019.

[140] V. Wallqvist, G. Kjell, E. Cupina, L. Kraft, C. Deck, and R. Willinger, “New functional pavements for pedestrians and cyclists,” *Accid. Anal. Prev.*, vol. 105, no. May, pp. 52–63, Aug. 2017.

[141] Klaus-Jurgen Bathe, *Finite Element Procedures*. Prentice-Hall Inc, 2003.

[142] W. S. Slaughter, *The Linearized Theory of Elasticity*. Boston, MA: Birkhäuser Boston, 2002.

[143] LSTC, *LS-DYNA R12 Keywords Manual, version 971*, vol. II. LIVERMORE SOFTWARE TECHNOLOGY (LST), AN ANSYS COMPANY, 2020.

[144] L. Khorashadi, J. M. Petscavage, and M. L. Richardson, "Postpartum symphysis pubis diastasis," *Radiol. Case Reports*, vol. 6, no. 3, p. 542, 2011.

[145] A. Pedrazzini, R. Bisaschi, R. Borzoni, D. Simonini, and A. Guardoli, "Post partum diastasis of the pubic symphysis: A case report," *Acta Biomed. l'Ateneo Parm.*, vol. 76, no. 1, pp. 49–52, 2005.

[146] K. A. Athanasiou, A. Agarwal, and F. J. Dzida, "Comparative study of the intrinsic mechanical properties of the human acetabular and femoral head cartilage," *J. Orthop. Res.*, vol. 12, no. 3, pp. 340–349, 1994.

[147] A. E. Anderson, B. J. Ellis, S. A. Maas, and J. A. Weiss, "Effects of idealized joint geometry on finite element predictions of cartilage contact stresses in the hip," *J. Biomech.*, 2010.

[148] J. Li, T. D. Stewart, Z. Jin, R. K. Wilcox, and J. Fisher, "The influence of size, clearance, cartilage properties, thickness and hemiarthroplasty on the contact mechanics of the hip joint with biphasic layers," *J. Biomech.*, vol. 46, no. 10, pp. 1641–1647, 2013.

[149] R. Ogden, *Non-linear elastic deformations*. 1984.

[150] R. S. Rivlin, "Large elastic deformations of isotropic materials IV. further developments of the general theory," *Philos. Trans. R. Soc. London. Ser. A, Math. Phys. Sci.*, vol. 241, no. 835, pp. 379–397, Oct. 1948.

[151] Y.-C. Fung, *Biomechanics*. New York, NY: Springer New York, 1993.

[152] SIS, *Standard - Impact attenuating playground surfacing - Methods of test for determination of impact attenuation SS-EN 1177:2018+AC*. 2019.

[153] X. Li and S. Kleiven, "Improved safety standards are needed to better protect younger children at playgrounds," *Sci. Rep.*, vol. 8Li, X., K, no. 1, pp. 1–12, 2018.

[154] T. J. Huang and L. T. Chang, "Design and evaluation of shock-absorbing rubber tile for playground safety," *Mater. Des.*, vol. 30, no. 9, pp. 3819–3823, 2009.

[155] M. Sadighi and S. J. Salami, "An investigation on low-velocity impact response of elastomeric & crushable foams," *Cent. Eur. J. Eng.*, vol. 2, no. 4, pp. 627–637, Dec. 2012.

[156] P. Sahandifar, S. Kleiven, and V. Wallqvist, "The risk of hip fracture is reduced around 40 percent for elderly men and women with a compliant pavement," *manuscript*, 2022.

[157] S. Kleiven and P. Sahandifar, "Upright trunk and slight anterior rotation of the pelvis cause the highest proximal femur forces during sideways falls," *Heliyon, Submitt.*, 2022.

[158] P. Sahandifar *et al.*, "A rubberized impact absorbing pavement can reduce the head injury risk in vulnerable road users: a bicycle and a pedestrian accident case study," *Traffic Inj. Prev.*, 2022.

[159] A. J. van den Kroonenberg, W. C. Hayes, and T. A. McMahon, "Dynamic Models for Sideways Falls From Standing Height," *J. Biomech. Eng.*, vol. 117, no. 3, pp. 309–318, Aug. 1995.

[160] M. N. Sarvi and Y. Luo, “Improving the prediction of sideways fall-induced impact force for women by developing a female-specific equation,” *J. Biomech.*, vol. 88, pp. 64–71, May 2019.

[161] P. M. de Bakker, S. L. Manske, V. Ebacher, T. R. Oxland, P. A. Cripton, and P. Guy, “During sideways falls proximal femur fractures initiate in the superolateral cortex: Evidence from high-speed video of simulated fractures,” *J. Biomech.*, vol. 42, no. 12, pp. 1917–25, Aug. 2009.

[162] S. L. Manske *et al.*, “Femoral neck cortical geometry measured with magnetic resonance imaging is associated with proximal femur strength,” *Osteoporos. Int.*, vol. 17, no. 10, pp. 1539–1545, Oct. 2006.

[163] E. Seeman, “During aging, men lose less bone than women because they gain more periosteal bone, not because they resorb less endosteal bone.,” *Calcif. Tissue Int.*, vol. 69, no. 4, pp. 205–8, Oct. 2001.

[164] T. M. Keaveny *et al.*, “Age-dependence of femoral strength in white women and men,” *J. Bone Miner. Res.*, vol. 25, no. 5, pp. 994–1001, 2010.

[165] S. Nawathe, H. Yang, A. J. Fields, M. L. Bouxsein, and T. M. Keaveny, “Theoretical effects of fully ductile versus fully brittle behaviors of bone tissue on the strength of the human proximal femur and vertebral body,” *J. Biomech.*, vol. 48, no. 7, pp. 1264–1269, May 2015.

[166] P. Zioupos and J. . Currey, “Changes in the Stiffness, Strength, and Toughness of Human Cortical Bone With Age,” *Bone*, vol. 22, no. 1, pp. 57–66, Jan. 1998.

[167] J. S. Bauer, S. Kohlmann, F. Eckstein, D. Mueller, E. M. Lochmüller, and T. M. Link, “Structural analysis of trabecular bone of the proximal femur using multislice computed tomography: a comparison with dual X-ray absorptiometry for predicting biomechanical strength in vitro.,” *Calcif. Tissue Int.*, vol. 78, no. 2, pp. 78–89, 2006.

[168] T. F. Lang *et al.*, “Age-related loss of proximal femoral strength in elderly men and women: The Age Gene/Environment Susceptibility Study - Reykjavik,” *Bone*, vol. 50, no. 3, pp. 743–748, Mar. 2012.

[169] M. Fahlstedt, S. Kleiven, and X. Li, “Current playground surface test standards underestimate brain injury risk for children,” *J. Biomech.*, vol. 89, pp. 1–10, 2019.

[170] X. G. Cheng *et al.*, “Assessment of the strength of proximal femur in vitro: Relationship to femoral bone mineral density and femoral geometry,” *Bone*, vol. 20, no. 3, pp. 213–218, 1997.

[171] E. M. M. Lochmüller, O. Groll, V. Kuhn, and F. Eckstein, “Mechanical strength of the proximal femur as predicted from geometric and densitometric bone properties at the lower limb versus the distal radius,” *Bone*, vol. 30, no. 1, pp. 207–216, 2002.

[172] M. L. Bouxsein, P. Szulc, F. Munoz, E. Thrall, E. Sornay-Rendu, and P. D. Delmas, “Contribution of trochanteric soft tissues to fall force estimates, the factor of risk, and prediction of hip fracture risk,” *J. Bone Miner. Res.*, vol. 22, no. 6, pp. 825–831, 2007.

[173] O. Ariza *et al.*, “Comparison of explicit finite element and mechanical simulation of the proximal femur during dynamic drop-tower testing,” *J. Biomech.*, vol. 48, no. 2, pp. 224–232, Jan. 2015.

[174] W. S. Enns-Bray *et al.*, “Material mapping strategy to improve the predicted response of the proximal femur to a sideways fall impact,” *J. Mech. Behav. Biomed. Mater.*, vol. 78, pp. 196–205, Feb. 2018.

[175] L. Grassi, S. P. Väänänen, M. Ristinmaa, J. S. Jurvelin, and H. Isaksson, "How accurately can subject-specific finite element models predict strains and strength of human femora? Investigation using full-field measurements," *J. Biomech.*, vol. 49, no. 5, pp. 802–806, 2016.

[176] K. T. Lim and W. J. Choi, "Effect of fall characteristics on the severity of hip impact during a fall on the ground from standing height," *Osteoporos. Int.*, 2020.